

**Journal of Biomechanics**  
**Patient-Specific Finite Element Analysis of Heart Failure: Mitral Valve Replacement and Tricuspid Valve Repair**  
--Manuscript Draft--

<b>Manuscript Number:</b>	
<b>Article Type:</b>	Full Length Article (max 3500 words)
<b>Keywords:</b>	Mitral Valve Regurgitation, Tricuspid Valve Repair, Heart Failure, Annuloplasty Ring, Finite Element Analysis
<b>Corresponding Author:</b>	Alireza Heidari, PhD McGill University Montreal, QC CANADA
<b>First Author:</b>	Yousof M.A. ABDEL-RAOUF, Master Student (Graduated)
<b>Order of Authors:</b>	Yousof M.A. ABDEL-RAOUF, Master Student (Graduated)  Alireza Heidari, PhD  Khalil EIKHODARY, Associate Professor  Mohamed BADRAN, PhD - Assistant Professor  Hojatollah VALI, PhD - Professor  Masoud ASGHARIAN, PhD - Professor  Antony A. YOUSSEF, Student  Cristina POP, Student  Dominique SHUM-TIM, Professor, M.D.,C.M., MSc., CPSQ., FRCSC., FAHA.,
<b>Abstract:</b>	Tricuspid annuloplasty is often recommended to mitigate the possible onset of right-sided heart failure in patients presenting with annular dilatation or tricuspid valve regurgitation (TR). This is an underreported clinical issue, especially when tricuspid valve (TV) failure occurs following invasive and non-invasive interventions such as mitral valve replacement or commissurotomy. We present the case of a 72-year-old female patient with severe mitral valve regurgitation who underwent mitral valve replacement, and we demonstrate the computational model used to predict the necessity of a tricuspid annuloplasty in addressing the possible development of secondary tricuspid regurgitation. A full-heart electro-mechanical finite element model was used to simulate the patient's heart based on magnetic resonance imaging (MRI) images prior to surgery and 3 days following surgery. Comparison of patient geometry pre-operation and post-operation showed a change in shape of the TV in systole. A rigid constraint across the TV annulus (TA) was used to simulate an annuloplasty ring. The desirable increase in ring-widening forces is predicted post-operation, with a significant reduction in contractile forces being exerted on the ring. Our model leads us to conclude that the patient will likely develop TV annular dilatation and subsequent regurgitation in the absence of further surgical intervention. We further highlight a general need to investigate by means of patient-specific <i>in silico</i> models valvular features in patients presenting with left-sided valvular disease, as computational modeling has greatly enhanced our ability to study their associated phenomena with more scrutiny and in real time. Such models have the potential to allow physicians better pre-surgical planning and prediction of short- and long-term patient outcomes.



**Alireza Heidari, Ph.D.**

Research Associate.

Department of Mathematics and Statistics, Faculty of Science

Department of Anatomy and Cell Biology, Faculty of Medicine

Tel: (514) 962-2600

Fax: (514) 398-5047

alireza.heidari@mcgill.ca

McGill University  
Burnside Hall, #1244  
805 Sherbrooke Street West  
Montreal, QC, H3A 0B9, Canada

July 17, 2020

Editor-in-Chief,  
Journal of Biomechanics

Dear Professor Guilak,

Attached please find my manuscript entitled "Patient-Specific Finite Element Analysis of the Human Heart: Mitral Valve Replacement and Tricuspid Valve Repair" co-authored by Yousof M.A. Abdel-Raouf, Alireza Heidari, Khalil Elkhodary, Mohamed Badran, Hojatollah Vali, Masoud Asgharian, Antony A. Youssef, Cristina Pop, Dominique Shum-Tim, that is submitted for possible publication in the Journal of Biomechanics .

Our manuscript presents, for the first time, a prospective study of modelling of the heart a patient with functional tricuspid regurgitation (FTR), pre- and post-surgery. Building on the generic living human heart model (LHHM), we have developed methods for adapting this generic model to make patient-specific heart models and prospectively follow clinical procedure. We illustrate our method using the MRI reports and images of a 72-year-old female patient with severe mitral valve regurgitation who underwent mitral valve replacement. We compare some important measures obtained from our model with those of our patient in her MRI report. The measured criteria using our model are strikingly close to the corresponding values in the MRI report, attesting to our claim that our model correctly represent the heart of our patient. Having established this confirmatory step, we have predicted the TV failure following surgical procedures on the left side of the heart for Mitral Valve Replacement. Our study demonstrates a computational method that can be turned into a decision-making support tool for medical practitioners to use with FTR and TV repair.

I also confirm that the manuscript, including related data, figures and tables has not been previously published and that the manuscript is not under consideration elsewhere.

Best regards,

A handwritten signature in blue ink, appearing to read "A.H." followed by a stylized surname.

Alireza Heidari, PhD,  
(on behalf of the authors).



**Alireza Heidari, Ph.D.**

Research Associate.

Department of Mathematics and Statistics, Faculty of Science

Department of Anatomy and Cell Biology, Faculty of Medicine

Tel: (514) 962-2600

Fax: (514) 398-5047

alireza.heidari@mcgill.ca

McGill University  
Burnside Hall, #1244  
805 Sherbrooke Street West  
Montreal, QC, H3A 0B9, Canada

July 15, 2020

**RE: Consent for article submission**

Dear Editor(s),

This letter is to confirm that I agree to be a corresponding author, to submit the attached manuscript entitled: "**Patient-specific Finite Element Analysis of the Human Heart: Mitral valve replacement and Tricuspid valve repair**" for consideration of publication in the **Journal of Biomechanics**. I also confirm that there are no conflict of interest, financial or otherwise, concerning the research involved with our manuscript.

I also acknowledge all our co-authors for their contributions in this paper from one direction to another.

Sincerely yours,

A handwritten signature in blue ink, appearing to read "A.H." followed by a stylized surname.

Alireza Heidari, Ph.D.



Hojatollah Vali, Ph.D.

Professor of Biomineralogy,  
Department of Anatomy & Cell Biology,  
Director, Emeritus  
Facility for Electron Microscopy Research  
McGill University

Tel: (514) 398-3025  
Fax: (514) 398-5047  
[hojatollah.vali@mcgill.ca](mailto:hojatollah.vali@mcgill.ca)

July 16, 2020

Ref.: Letter of Agreement

To whom it may concern,

This is to confirm that I agree with the submission of the manuscript entitled "*Patient-Specific Finite Element Analysis of the Human Heart: Mitral Valve Replacement and Tricuspid Valve Repair*" to the Journal of Biomechanics.

I also confirm that there are no conflict of interest concerning the research involved with this manuscript

Sincerely yours,

A handwritten signature in black ink, appearing to read "H. Vali".

Hojatollah Vali



**Dominique Shum-Tim, M.D., C.M., M.Sc., C.S.P.Q., F.R.C.S.C., F.A.C.S., F.A.H.A., F.C.C.S.**

Professeur

Division de la Chirurgie Cardiaque

Université McGill

Tel : (514) 934-1934 ext. 36873

Professor

Division of Cardiac Surgery

McGill University

Fax : (514) 843-1602

July 16<sup>th</sup>, 2020.

**Re: Letter of agreement**

Dear Editor,

This letter is to notify my agreement as a co-author, to submit the attached manuscript entitled: "**Patient-specific Finite Element Analysis of the Human Heart: Mitral valve replacement and Tricuspid valve repair**" for consideration of publication in the **Journal of Biomechanics**. I, hereby, declared that I have no conflict of interest, financial or otherwise.

I also acknowledge the contributions of each and every one of the co-authors in this paper for their valuable opinions and suggestions.

Yours sincerely,

A handwritten signature in blue ink, appearing to read "D. Shum-Tim".

D. Shum-Tim, M.D., C.M., MSc., CPSQ., FRCSC., FAHA., FACS., FCCS.  
Professor,  
Department of Surgery  
Department of Pediatric Surgery  
McGill University Health Center  
McGill University  
1001 Decarie Boulevard,  
Room C 07.1284.5  
Montreal, Quebec,  
Canada, H4A 3J1  
Tel: 514-934-1934 x36873  
Fax: 514-843-1602

July 13, 2020.

Re: Letter of agreement

Dear Editor,

I am writing this letter to document my agreement as a co-author to the submission entitled **“Patient-specific Finite Element Analysis of the Human Heart: Mitral valve replacement and Tricuspid valve repair”** for publication in the **Journal of Biomechanics (Elsevier)**. I, hereby, declare that I have no conflict of interest, financial or otherwise.

Yours sincerely,

Cristina Pop, M.D., C.M. candidate  
Department of Medicine  
Faculty of Medicine  
McGill University

A handwritten signature in black ink that reads "Cristina Pop".

### Letter of Agreement

Dear Editor,

This letter is to notify my agreement as a co-author, to submit the attached manuscript entitled: "**Patient-specific Finite Element Analysis of the Human Heart: Mitral valve replacement and Tricuspid valve repair**" for consideration of publication in the **Journal of Biomechanics**. I, hereby, declare that I have no conflict of interest, financial or otherwise.



Khalil I. Elkhodary

Associate Professor of Computational Mechanics  
The Department of Mechanical Engineering  
The American University in Cairo

**Letter of Agreement**

Dear Editor,

This letter is to notify my agreement as a co-author, to submit the attached manuscript entitled: "**Patient-specific Finite Element Analysis of the Human Heart: Mitral valve replacement and Tricuspid valve repair**" for consideration of publication in the **Journal of Biomechanics**. I, hereby, declare that I have no conflict of interest, financial or otherwise.

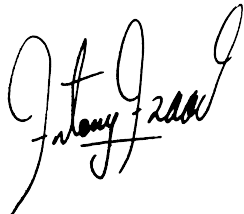


Yousof Abdel-Raouf  
Graduate Student & Research Assistant  
The Department of Mechanical Engineering  
The American University in Cairo

**Letter of Agreement**

Dear Editor,

This letter is to notify my agreement as a co-author, to submit the attached manuscript entitled: "**Patient-specific Finite Element Analysis of the Human Heart: Mitral valve replacement and Tricuspid valve repair**" for consideration of publication in the **Journal of Biomechanics**. I, hereby, declare that I have no conflict of interest, financial or otherwise.



Antony Youssef  
Research Assistant  
The Department of Mechanical Engineering  
The American University in Cairo

**Letter of Agreement**

July 13, 2020

I would like to state as co-author that I agree on submitting the paper entitled "**Patient-Specific Finite Element Analysis of the Human Heart: Mitral Valve Replacement and Tricuspid Valve Repair**" to the Journal "**Journal of Biomechanics**".

I also certify that I have no conflict of interest either financial or otherwise.

Mohamed Badran, PhD.



Assistant Professor  
Mechanical Engineering Department  
Faculty of Engineering and Technology  
Future University in Egypt



Masoud Asgharian, PhD  
Full Professor  
Department of Mathematics and Statistics  
Burnside Hall, Room 1224  
805 Sherbrooke Street West  
Montreal, QC, Canada, H3A 0B9  
[masoud.asgharian2@mcgill.ca](mailto:masoud.asgharian2@mcgill.ca)

The Editor(s) of the *Biomechanics* journal

July 12, 2020

**RE: Consent for article submission**

Dear Editor(s),

I am writing to document my consent to the submission of our manuscript entitled "*Patient-Specific Finite Element Analysis of the Human Heart: Mitral Valve Replacement and Tricuspid Valve Repair*" to the *Biomechanics* journal. Further to my consent for submitting the aforementioned article by Dr. A. Heidari, I add that I have no conflict of interest, financial or otherwise.

Sincerely,

A handwritten signature in black ink, appearing to read "Masoud Asgharian".

Masoud Asgharian

**Suggested reviewers:**

**Dr. Steven M Levine, PhD**

Executive Director,

Living Heart Project

Dassault Systèmes

+1 401-368-5178

[Steven.LEVINE@3ds.com](mailto:Steven.LEVINE@3ds.com)

**Professor Stanley Nattel, MD**

Cardiologist, Montreal Heart Institute

Professor of Medicine, University of Montreal

+1 514-376-3330 Ext 3990

[stanley.nattel@icm-mhi.org](mailto:stanley.nattel@icm-mhi.org)

**DR. Kinda Khalaf, PhD**

Associate Professor and Associate Chair

Department of Biomedical Engineering

Address: P.O. Box 127788, Abu Dhabi, UAE

Telephone: +971-(0)2-4018107

Fax: +971-(0)2-4472442

Email: [kinda.khalaf@ku.ac.ae](mailto:kinda.khalaf@ku.ac.ae)

# Patient-Specific Finite Element Analysis of Heart Failure: Mitral Valve Replacement and Tricuspid Valve Repair

Yousof M.A. ABDEL-RAOUF<sup>1</sup>, Alireza HEIDARI<sup>2,3\*</sup>, Khalil ELKHODARY<sup>1</sup>, Mohamed BADRAN<sup>4</sup>, Hojatollah VALI<sup>3</sup>, Masoud ASGHARIAN<sup>2</sup>, Antony A. YOUSSEF<sup>1</sup>, Cristina POP<sup>5</sup>, Dominique SHUM-TIM<sup>6</sup>

<sup>1</sup> Department of Mechanical Engineering, American University in Cairo, 11835, New Cairo, Egypt

<sup>2</sup> Department of Mathematics and Statistics, McGill University, Montreal, QC, H3A 0B9, Canada

<sup>3</sup> Department of Anatomy and cell biology, McGill University, Montreal, QC, H3A 0B9, Canada

<sup>4</sup>Mechanical Engineering Department, Future University in Egypt, 11835, New Cairo, Egypt

<sup>5</sup>Department of Medicine, Faculty of Medicine, McGill University. Montreal, Canada

<sup>6</sup>Department of Surgery, McGill University Health Center, Montreal, QC, H4A 3J1, Canada

\*Corresponding author. Email Address: alireza.heidari@mcgill.ca

Tel: + 1-514-962-2600; fax: +1-514-398-5047

Submitted: July 17, 2020

Word Count: 2888

**Keywords:** Mitral Valve Regurgitation, Tricuspid Valve Repair, Heart Failure, Annuloplasty Ring, Finite Element Analysis.

## Abstract

Tricuspid annuloplasty is often recommended to mitigate the possible onset of right-sided heart failure in patients presenting with annular dilatation or tricuspid valve regurgitation (TR). This is an underreported clinical issue, especially when tricuspid valve (TV) failure occurs following invasive and non-invasive interventions such as mitral valve replacement or commissurotomy. We present the case of a 72-year-old female patient with severe mitral valve regurgitation who underwent mitral valve replacement, and we demonstrate the computational model used to predict the necessity of a tricuspid annuloplasty in addressing the possible development of secondary tricuspid regurgitation. A full-heart electro-mechanical finite element model was used to simulate the patient's heart based on magnetic resonance imaging (MRI) images prior to surgery and 3 days following surgery. Comparison of patient geometry pre-operation and post-operation showed a change in shape of the TV in systole. A rigid constraint across the TV annulus (TA) was used to simulate an annuloplasty ring. The desirable increase in ring-widening forces is

predicted post-operation, with a significant reduction in contractile forces being exerted on the ring. Our model leads us to conclude that the patient will likely develop TV annular dilatation and subsequent regurgitation in the absence of further surgical intervention. We further highlight a general need to investigate by means of patient-specific in silico models valvular features in patients presenting with left-sided valvular disease, as computational modeling has greatly enhanced our ability to study their associated phenomena with more scrutiny and in real time. Such models have the potential to allow physicians better pre-surgical planning and prediction of short- and long-term patient outcomes.

# Patient-Specific Finite Element Analysis of Heart Failure: Mitral Valve Replacement and Tricuspid Valve Repair

Yousof M.A. ABDEL-RAOUF<sup>1</sup>, Alireza HEIDARI<sup>2,3\*</sup>, Khalil ELKHODARY<sup>1</sup>, Mohamed BADRAN<sup>4</sup>, Hojatollah VALI<sup>3</sup>, Masoud ASGHARIAN<sup>2</sup>, Antony A. YOUSSEF<sup>1</sup>, Cristina POP<sup>5</sup>, Dominique SHUM-TIM<sup>6</sup>

<sup>1</sup> Department of Mechanical Engineering, American University in Cairo, 11835, New Cairo, Egypt

<sup>2</sup> Department of Mathematics and Statistics, McGill University, Montreal, QC, H3A 0B9, Canada

<sup>3</sup> Department of Anatomy and cell biology, McGill University, Montreal, QC, H3A 0B9, Canada

<sup>4</sup>Mechanical Engineering Department, Future University in Egypt, 11835, New Cairo, Egypt

<sup>5</sup>Department of Medicine, Faculty of Medicine, McGill University. Montreal, Canada

<sup>6</sup>Department of Surgery, McGill University Health Center, Montreal, QC, H4A 3J1, Canada

\*Corresponding author. Email Address: alireza.heidari@mcgill.ca

Tel: + 1-514-962-2600; fax: +1-514-398-5047

Submitted: July 17, 2020

Word Count: 2888

**Keywords:** Mitral Valve Regurgitation, Tricuspid Valve Repair, Heart Failure, Annuloplasty Ring, Finite Element Analysis.

## Abstract

Tricuspid annuloplasty is often recommended to mitigate the possible onset of right-sided heart failure in patients presenting with annular dilatation or tricuspid valve regurgitation (TR). This is an underreported clinical issue, especially when tricuspid valve (TV) failure occurs following invasive and non-invasive interventions such as mitral valve replacement or commissurotomy. We present the case of a 72-year-old female patient with severe mitral valve regurgitation who underwent mitral valve replacement, and we demonstrate the computational model used to predict the necessity of a tricuspid annuloplasty in addressing the possible development of secondary tricuspid regurgitation. A full-heart electro-mechanical finite element model was used to simulate the patient's heart based on magnetic resonance imaging (MRI) images prior to surgery and 3 days following surgery. Comparison of patient geometry pre-operation and post-operation showed a change in shape of the TV in systole. A rigid constraint across the TV annulus (TA) was used to simulate an annuloplasty ring. The desirable increase in ring-widening forces is

34 predicted post-operation, with a significant reduction in contractile forces being exerted on the ring. Our  
35 model leads us to conclude that the patient will likely develop TV annular dilatation and subsequent  
36 regurgitation in the absence of further surgical intervention. We further highlight a general need to  
37 investigate by means of patient-specific in silico models valvular features in patients presenting with left-  
38 sided valvular disease, as computational modeling has greatly enhanced our ability to study their  
39 associated phenomena with more scrutiny and in real time. Such models have the potential to allow  
40 physicians better pre-surgical planning and prediction of short- and long-term patient outcomes.

41 **1. Introduction**

42 Mitral Valve Regurgitation (MR) is a valvular disease affecting approximately 0.59% of adults and with  
43 its prevalence increasing significantly with age (Dziadko and Enriquez-Sarano, 2016). MR is associated  
44 with Left Ventricular (LV) dysfunction, is characterized by incomplete Mitral Valve (MV) leaflet  
45 coaptation, and in severe cases leads to Heart Failure (HF). It is also a major factor in the onset of  
46 Pulmonary Hypertension (PH), creating a higher RV afterload, ultimately causing Right Ventricular (RV)  
47 dilation, Tricuspid annulus (TA) dilation and secondary Tricuspid Valve Regurgitation (TR) (Badano et  
48 al., 2013). This is also termed Functional TR (FTR) and occurs in approximately 30% to 50% of those with  
49 severe MR (Cohen et al., 1987; Koelling et al., 2002), with incidences of severe FTR in approximately 14%  
50 of patients who underwent MV replacement (Izumi et al., 2002).

51 While common for patients with severe MR to undergo MV replacement surgery, assessment of FTR  
52 and agreement on intervention and its necessity, in the form of TV annuloplasty varies among experts in  
53 the cardiologist community (David et al., 2015; Shuhaiher, 2018), with many drafting different guidelines  
54 to help classify patients and their respective intervention policies (Dreyfus et al., 2015; Verdonk et al.,  
55 2018). Many procedures regarding repair of the TV exist, including the suturing of two TV leaflets at the  
56 middle of their edges called the “clover” technique (Bellushi et al., 2018), and recently the adaptation of  
57 an intervention previously used to treat regurgitant MV leaflets by pinching them together using a device  
58 named MitralClip (Dabiri et al., 2019). On the other hand, the De Vega technique involves the suture of  
59 components of the TA (Wei et al., 1993), and the use of annuloplasty rings, first employed by (Carpentier  
60 et al., 1971), has become a popular choice for valve repair. Both rigid and semi-rigid rings can be used and

61 the choice between them will determine the amount of TA remodeling, although care must be given to the  
62 cardiac tissue's ability to withstand the large cyclical forces (Pfannmüller et al., 2012).

63 With the recent increase of computational tools, attention has been given to creating computational  
64 models of the heart that reflect anatomical and physiological diseases which lend insight into relevant  
65 pathophysiology, complications and intervention policies. For instance, (Shalaby et al., 2019) investigate  
66 computationally the complications that arise from drug cardiotoxicity, as reflected in distorted ECGs,  
67 altered cardiac function. Additionally, computational studies serve as a decision-making aid to questions  
68 where there is no established clinical consensus on assessment and intervention policies. Work by  
69 (Rahmani et al., 2019) leverages such tools in predicting the subclavian steal syndrome (SSS) occurrence  
70 in haemodialysis patients undergoing coronary artery bypass (CABG) by assessing the arterial stenosis.  
71 They were able to determine a threshold of stenosis at 54% beyond which retrograde flow in the  
72 subclavian artery would lead to the steal phenomenon and computational modelling was the only method  
73 to quantitatively investigate it. Previous work highlighting the effect of novel annuloplasty on regurgitant  
74 MV has been presented (Baillargeon et al., 2015). More recent work focused on Finite Element (FE) TV  
75 modelling and presents patient-specific dynamics of healthy TV geometry obtained using Multi-sliced  
76 computer tomography (MSCT), and a hyperelastic formulation for the material response (Kong et al.,  
77 2018). A subsequent analysis by (Singh-Gryzbon et al., 2019) addressed some of the assumptions made in  
78 (Kong et al., 2018) regarding chordae tendinea and papillary muscle locations, by setting up an  
79 experimental framework to capture TV-chordae geometry, while employing Fluid Structure Interaction  
80 (FSI) to computationally determine the effect of TR on hemodynamic. Most recently, (Dabiri et al., 2019)  
81 have used FSI to demonstrate the application of MitraClip, and its ability to reduce regurgitation in the  
82 TV. Highlighting the interplay between RV dynamics and the TV will greatly add to our understanding of  
83 the etiology and intervention policies pertaining to FTR, especially since FTR is a product of RV failure or  
84 remodelling (Lee et al., 2019; Morgan et al., 2019). To our knowledge that there has not been any full  
85 heart computational modelling which investigates this important issue.

86 To that end, we present herein the case of a 72-year-old female symptomatic with chest pain and  
87 exertional dyspnea, suffering severe MVR, PH and Left Atrial (LA) dilation. Based on the benefits that  
88 tissue-based valves afford patients (Le Huu and Shum-Tim, 2014), it was concluded that the patient  
89 would undergo MV replacement using a bioprosthetic valve. We present a simulation of the full patient

90 heart before and after surgery using the (FE) method in which we examine the ventricle-valve dynamics.  
91 We also simulate the presence of a TV annuloplasty ring to demonstrate that if annuloplasty is not  
92 undertaken it is predicted that the patient post MV-replacement surgery will nonetheless likely develop  
93 FTR and RV failure due to excessive cyclical forces on the annulus that lead to Tricuspid Annulus (TA)  
94 dilation.

95 **2. Methodology**

96 *2.1. Patient Specification*

97 A patient-specific geometry and corresponding cardiac function were obtained from a transthoracic  
98 echocardiogram (TTE) and cardiac magnetic resonance (CMR) (**Fig. 1**). The patient underwent  
99 bioprosthetic mitral valve replacement (Biologic Epic #29) (Abbott Laboratories, Chicago, IL, USA) and  
100 tricuspid valve repair (Ring #30) at Tehran Heart Center, Iran. While transcatheter deployment of the  
101 artificial valve presented a less invasive option (Le Huu and Shum-Tim, 2020), the patient underwent  
102 open-heart surgery due to tricuspid valve repair. Patient underwent surgical management as determined  
103 by the surgical team at the Tehran Heart Center as per the most recent guidelines. Patient-specific  
104 simulation using computational modeling was done in a prospective matter, such that imaging was  
105 performed, and medical records were obtained throughout the patient's management without interference  
106 with the pre-established treatment.

107 CMR imaging was acquired by multi-planar MR sequences using true fast imaging with steady state  
108 procession (truFISP), truFISP cine, whole heart coronary imaging, and 3D contrast-enhanced high-  
109 resolution MR angiography (MRA) of the vessels of the chest and upper abdomen with administration of  
110 20 ml of Gadolinium contrast agent.

111 *2.2. Simulation*

112 We begin with an initial geometry, i.e. an idealized 3D CAD heart model (Zygote Media Group Inc.,  
113 American Fork, UT, USA). We modified this initial geometry by adopting a dilation-based morphing  
114 method and reshaped the cardiac chambers into the dilated states which corresponded to patient geometry  
115 (Athanasios, 2019). Heart remodeling before and after surgery was thus simulated.

116 The network of Purkinje fibers corresponding to our patient is composed of 3D truss elements, in a  
117 fractal pattern, spanning the endocardium (Sahli et al., 2016). In order to morph these fibers according to

118 patient's ventricular geometries, a zero-distance mapping constraint described in Eqn. 1 was enforced  
 119 between Purkinje nodes and ventricular nodes.

$$120 P(x,y,z) - N(x,y,z) = P'(x,y,z) - N'(x,y,z), \quad (1)$$

121 Where  $P(x,y,z)$  and  $P'(x,y,z)$  correspond to the initial Purkinje fiber nodal coordinates and morphed  
 122 coordinates respectively, and  $N(x,y,z)$  and  $N'(x,y,z)$  correspond to the nearest initial ventricular nodal  
 123 coordinates and morphed nodal coordinates respectively. A schematic of the adjustment methodology is  
 124 shown in **Fig. 2**.

125 We further simulated for three cardiac cycles the mechanical response of the remodeled geometries on  
 126 the Living Heart Human Model (LHHM) in Abaqus 2019 (Baillargeon et al., 2014). In the LHHM, the  
 127 atria and ventricles have been discretized into 263,028 3D deformable linear tetrahedral elements.  
 128 Ventricular fiber orientations are applied to element centroids in accordance to the method of (Streeter et  
 129 al., 1969), while atrial fiber orientations are assigned in correspondence to the findings of the euroHeart  
 130 project (Weese et al., 2007).

131 The passive response of the chambers is modeled as incompressible, anisotropic, and hyperelastic, as  
 132 given by the Strain Energy Function (Holzapfel and Ogden, 2009):

$$133 \Psi_{deviatoric} = \frac{a}{2b} e^{b(I_1 - 3)} + \sum_{i=f,s} \frac{a_i}{2b_i} (e^{b_i(I_{4i} - 1)^2} - 1) + \frac{a_{fs}}{2b_{fs}} (e^{b_{fs}(I_{8fs})^2} - 1), \quad (2)$$

$$134 \Psi_{volumetric} = \frac{1}{D} \left( \frac{J^2 - 1}{2} - \ln(J) \right), \quad (3)$$

135 Where  $a$ ,  $b$ ,  $a_f$ ,  $a_s$ ,  $a_{fs}$  and  $b_{fs}$  are material constants. The value of  $I_1$  describes the isotropic response and  
 136 is the first principal invariant of the left Cauchy-Green tensor,  $\mathbf{C}$ , and is given by  $I_1 = \text{tr}(\mathbf{C})$ . The two  
 137 invariants that describe transversely isotropic behavior are  $I_{4f}$ ,  $I_{4s}$ , each being evaluated as  $\mathbf{f}_o \cdot (\mathbf{C} \mathbf{f}_o)$  and  
 138  $\mathbf{s}_o \cdot (\mathbf{C} \mathbf{s}_o)$  respectively. Finally, the orthotropic response is incorporated in the term  $I_{8fs} = \mathbf{f}_o \cdot (\mathbf{C} \mathbf{s}_o)$ . The  
 139 directions  $\mathbf{f}$  and  $\mathbf{s}$  are evaluated at any time as  $\mathbf{F} \mathbf{f}_o$  and  $\mathbf{F} \mathbf{s}_o$  where  $\mathbf{F}$ ,  $\mathbf{f}_o$  and  $\mathbf{s}_o$  are the deformation  
 140 gradient, fiber direction and sheet direction respectively. The volumetric response is composed of the bulk  
 141 modulus,  $D$ , and the Jacobian,  $J$ .

142 Conversely, an active material response reflecting the electrically sensitive tension along the myofibers,  
 143 as given by Walker et al. (Walker et al., 2004), is adopted:

$$144 \sigma(t, E_{ff})_{\text{active fiber}} = T_{\max} \frac{C a_0^2}{2(C a_0^2 + E C a_{50}^2)} (1 - \cos(\omega)), \quad (4a)$$

145  $ECa_{50} = \frac{Ca_{0\max}}{\sqrt{e^{B(l-l_0)} - 1}},$  (4b)

146  $\omega = \begin{cases} \pi \frac{t}{t_0}, & \text{when } 0 \leq t \leq t_0 \\ \pi \frac{t-t_0+t_r}{t_r}, & \text{when } t_0 \leq t \leq t_0 + t_r \\ 0, & \text{when } t_0 + t_r \leq t \end{cases}$

147 (4c)

148  $t_r = ml + b,$  (4d)

149  $l = l_r \sqrt{2E_{ff} + 1},$  (4e)

150 Where  $T_{max}$  is the maximum active stress in the fiber,  $Ca_0$  and  $Ca_{0\max}$  represent peak Calcium  
 151 concentration in the myofiber,  $l_0$  is the minimum sarcomere length at which active stress develops,  $l_0$  is  
 152 the initial fiber length,  $t_0$  is the time until maximum stress is reached,  $B$ ,  $m$  and  $b$  are phenomenological  
 153 constants and finally,  $E_{ff}$  is the Green-Lagrange strain component along the fiber direction.

154 The true stress along the fiber will therefore be

155  $\sigma_{fiber} = \sigma_{passive\ fiber} + \sigma_{active\ fiber},$  (5)

156 Fine tuning the aforementioned parameters was a necessary step to obtain the appropriate patient-  
 157 specific Ejection Fraction (EF) and to reflect the increase in stiffness associated with ageing described in  
 158 literature (Walker et al., 2005; Fujimoto et al., 2012).

159 ***2.3. FTR and Annuloplasty***

160 The TV and MV were discretized into denser meshes of 21,252 and 70,210 deformable 3D linear  
 161 tetrahedral elements respectively. Chordae were modeled as truss elements and chordae-TV interactions  
 162 and TV-RV interactions were defined by distributed coupling, and the chordae were fixed to the Papillary  
 163 Muscles (PM) using a tie-constraint (Abaqus Analysis User's Manual, 2014). The material constants used  
 164 in this work to describe the MV and TV have been also adjusted to represent the stresses described in  
 165 May-Newman and Yin (May-Neumann and Yin, 1995). Chordae and PM location have been adjusted to  
 166 simulate complete closure in the neutral RV geometry. The TA in our model is defined as the region of the  
 167 ventricles to which the valves are attached. Local fiber orientations of the valve and corresponding biaxial  
 168 data describing the isotropic Marlow hyperelastic material response of the chordae were adapted from  
 169 (Kunzleman and Cochran, 1990). It is also important to note that previous work has commented on the

170 mechanics of valve interstitial cells (VICs) which undergo unique viscoelastic dynamics (Sakamoto et al.,  
171 2017), and this has been overlooked in this work for simplicity. A 0D-Windkessel model was used to  
172 extract fluid pressure across the different cardiac chambers, and patient-specific transvalvular pressure  
173 was thus applied to the ventricular sides of the TV leaflets.

174 To model the post-operative geometry for the patient, their MV geometry must be forgone (due to the  
175 replacement). We instead model the effect of the replacement valve and ring using connector elements.  
176 This is done by constraining 20 nodes which substitute for suture points between the new ring/valve  
177 complex and the ventricles (Baillargeon et al., 2015). Each node is connected to its neighbor by a rigid link  
178 in a circumferential formation (**Fig. 3**) to remove relative motion between suture points, and to mimic the  
179 mechanical effect of the new ring/MV complex (Abaqus Analysis User's Manual, 2014).

180 Surgical intervention planning for TV repair requires a thorough understanding of the state of the TA. In  
181 order to study the behavior of the TA pre- and post-operatively, we further define a hypothetical ring as  
182 above for the TA, so that forces measured along the ring would directly reflect TA dynamics in the cardiac  
183 cycle. We assign wire connector elements that link 40 ventricular nodes along the TA, using rigid links to  
184 constrain their relative motion and to simulate the effect of a rigid annuloplasty ring. Average link length  
185 was  $3.74 \pm 1.22$  mm in the pre-operative geometry and  $4.07 \pm 2.44$  mm in the post-operative geometry.

186 We also explore the effect of using rigid and semi-rigid links on the forces in the TA for the post-operative  
187 geometry. In the semi-rigid case, axial connectors are prescribed an elasticity and a damping, as  
188 characteristic of the behavior of a spring-dashpot (Abaqus Analysis User's Manual, 2014). Resulting forces  
189 on these elements are compared to help elucidate the difference between forces on the TA before MV  
190 replacement and after.

191 **3. Results**

192 Pre-operatively, echocardiography and magnetic resonance imaging showed for the patient biatrial  
193 enlargement, while RV and LV size were within normal range. Velocity flow assessment showed severe  
194 mitral regurgitation, thickened leaflets, mild mitral stenosis (mitral valve area =  $1.8 \text{ cm}^2$ , mean gradient 5  
195 mmHg), and echocardiography showed Pulmonary arterial pressure was 70 mmHg, compared to 64  
196 mmHg upon right heart catheterization.

Following mitral valve replacement and tricuspid valve repair, a CMR was repeated for the patient. There was an estimated 15% reduction in LA, resulting in a 30% reduction in LA cavity volume, while the RA remained normal in size. Velocity flow mappings showed no mitral regurgitation, with a mild tricuspid regurgitation. There was a significant reduction in pulmonary hypertension to 30 mmHg on repeat TTE. There was persistent global LV and RV hypokinesis, which is compatible with chronic cardiac remodeling as seen with non-ischemic dilated cardiomyopathy (Huikiri, 1983; Gaasch and Meyer, 2008).

Dilated pre-operative patient volume and shape were simulated in our model, and an atrial view of the valves shows severe MR mid-systole (**Fig. 4**). We also simulated a reduced Tricuspid Annular Systolic Excursion (TAPSE), reporting a value of 13.78 mm. End diastolic (ED) TA diameter calculated from the septal segment to the lateral segment was  $46.24 \pm 5.26$  mm. Maximum principle stress was largest at the MV - aortic root, and maximum principle strain is largest at TV and MV leaflet bellies, with the largest strain being located in the Anterior Tricuspid Leaflet (ATL) compared to the other TV leaflets (**Fig. 5a,c**).

Modeled post-operative geometry also showed the remodeled TA to be more rounded, and that the ED TA annulus was reduced slightly to  $44.06 \pm 1.11$  mm. The replaced MV has noticeably decreased stress at the aortic root (**Fig. 5b**), as well as increased strain distribution across TV leaflets (**Fig. 5d**).

A comparison of the forces exerted by the TA showed post-operative TA to have a mildly higher force (~2 N) in diastole while pre-operative TA exhibited a remarkably larger force during the systolic phase (~42 N) (**Fig. 6**). The segments of TA experiencing the highest forces in the pre-operative geometry were located at the antero-lateral segment of the TA with a peak average force of  $2.990 \pm 0.038$  N, while post-operative geometry experiences the highest forces at the septal region with a peak average force of  $1.144 \pm 0.020$  N (**Fig. 7**).

After ascribing a spring-dashpot axial behavior to the links on the post-operative geometry, a significant reduction in total force was observed on contraction (**Fig. 8**). A breakdown of TA forces is shown in **Table 1**.

**Table 1** Breakdown of Total Forces on Pre-Operative and Post-Operative Geometries.

	Constraint Type	Max. (N)	Min. (N)	Average (N)
Pre-Operative	Rigid	65.54	1.38	12.05
	Rigid	21.67	3.06	7.50
Post-Operative	Semi-Rigid	17.39	2.77	6.48

222    **4. Discussion**

223    In this prospective study, we highlight the role of native geometry of the ventricles on valve dynamics.  
224    This is important to reflect valve diseases that do not result from leaflet abnormality but rather changes in  
225    the valve-chordae-ventricle complex. Patient geometry was replicated and TAPSE indicated reduced RV  
226    function and imminent RV failure (CME Exam for Guidelines, 2010; Modin et al., 2019). LA dilation in  
227    pre-operative geometry was the main cause of MVR in our model, demonstrating an accurate portrayal of  
228    left-side failure by our model. Additionally, RA dilation pre-operatively, and its size reduction post-  
229    operatively, created a TV diameter > 40 mm, which indicates the need for TV repair (Dreyfus et al., 2015;  
230    Verdonk et al., 2018). We herein report TV stresses and stress distributions in agreement with Kong et. al.  
231    (2018) and Singh-Gryzbon et al. (2019).

232    Analysis of the forces on TA suggest that during the cardiac cycle TA widening post operatively was  
233    larger, indicating that over time the TA would dilate. Moreover, TA contraction was shown to be  
234    significantly reduced post-operatively, indicating valve closure would be impaired with time. This, along  
235    with the enlarged TA diameter and the patient's MV replacement suggest the patient now presents the key  
236    markers for which the ACA/AHA guidelines recommend TV repair (ACC/AHA 2006 Guidelines, 2006).

237    In the comparison of rigid and semirigid rings, our model demonstrated notably larger forces on rigid  
238    constraints, which suggests a more likely failure mode in accordance with clinical findings (Pfannmüller  
239    et al., 2012). Hence, it seems advisable that a full description of the mechanical properties of ring  
240    material, be incorporated in the *in-silico* model, is necessary for further detail of the behavior of a selected  
241    annuloplasty ring during pre-operative planning.

242    Employing an idealized shape of the TV and MV instead of segmentation is a clear limitation of our  
243    approach in this manuscript; however, our focus is not to study valve behavior alone, but rather the  
244    behavior of the ventricle-valve-chordae complex, rendering our simplification an important expedience.  
245    Furthermore, the mechanical description of the TA in our model is also simplified, not taking into account  
246    the tiered nature of the TA which transitions from a cardiomyocyte-dominant tissue to a cell-free  
247    collagenous tissue. Lastly, our use of 40 nodes to corresponding to 40 sutures was not patient-specific, an  
248    assumption which affects the exact magnitudes of forces reported on the TA.

249     **5. Conclusion**

250         A computational model for the human heart is geometrically and functionally adapted to simulate  
251         a patient-specific heart, using magnetic resonance images before and three days after surgery. Our study  
252         demonstrates a computational method that can be turned into a decision-making support tool for medical  
253         practitioners to use with FTR and TV repair. We have shown our computational approach is capable of  
254         predicting TV failure following surgical procedures on the left side of the heart for Mitral Valve  
255         Replacement. Our approach can quantitatively study several scenarios for TV repair using ring  
256         annuloplasty, giving insight into forces and stresses that can be invaluable to the pursuit of better  
257         understanding of valve repair and its efficiency.

258     **Conflict of interest**

259         The authors wish to declare no conflict of interest.

260     **Acknowledgements**

261         YA wishes to gratefully acknowledge the support of the Al-Alfi Foundation through the AL-Alfi  
262         Graduate Studies Fellowship. AH would like to express his gratitude to the Iranian Elite Foundation and  
263         Tehran Heart Centre for their support at the early stages of this project as well as Dr. Sara Sheibani at  
264         McGill department of Anatomy and Cell Biology for technical support related to the physiological  
265         parameters in the model. MA's research is partly supported by NSERC Canada. The authors are grateful  
266         for the invaluable help and collaboration of the members of the Living Heart Project and their research  
267         team.

268

269 **References**

- 270 Abaqus Analysis User's manual, Dassault Systèmes, Simulia Corp. Version 6.14., Providence, RI,  
271 2014 .
- 272
- 273 ACC/AHA 2006 Guidelines for the Management of Patients with Valvular Heart Disease:  
274 Executive Summary. Circulation, 114(5), pp. 450-527, 2006. Available:10.1161/circulationaha.106.177303.
- 275
- 276 Athanasios, A., 2019. A computational model for dilated cardiomyopathy: morphology and  
277 electromechanics. M.Sc., Thesis, The American University in Cairo. Digital Archive and Research  
278 Repository (DAR).
- 279
- 280 Badano, L., Muraru, D. and Enriquez-Sarano, M., 2013. Assessment of functional tricuspid  
281 regurgitation. European Heart Journal, 34(25), pp.1875-1885. Available: 10.1093/eurheartj/ehs474.
- 282
- 283 Baillargeon, B., Rebelo, N., Fox, D., Taylor, R. and E. Kuhl, E., 2014. The Living Heart Project: A  
284 robust and integrative simulator for human heart function. European Journal of Mechanics - A/Solids,  
285 48, pp. 38-47. Available: 10.1016/j.euromechsol.2014.04.001.
- 286
- 287 Baillargeon, B., Costa, I., Leach, J., Lee, L., Genet, M., Toutain, A., Wenk, J., Rausch, M., Rebelo,  
288 N., Acevedo-Bolton, G., Kuhl, E., Navia, J. and Guccione, J., 2015. Human Cardiac Function Simulator for  
289 the Optimal Design of a Novel Annuloplasty Ring with a Sub-valvular Element for Correction of Ischemic  
290 Mitral Regurgitation. Cardiovascular Engineering and Technology, 6(2), pp.105-116. Available:  
291 10.1007/s13239-015-0216-z.
- 292
- 293 Belluschi, I., Del Forno, B., Lapenna, E., Nisi, T., Iaci, G., Ferrara, D., Castiglioni, A., Alfieri, O.  
294 and De Bonis, M., 2018. Surgical Techniques for Tricuspid Valve Disease. Frontiers in Cardiovascular  
295 Medicine, 5. Available: 10.3389/fcvm.2018.00118.
- 296
- 297 Carpenter, A., Deloche, A., Dauptain, J., Soyer, R., Blondeau, P., Piwnica, A., Dubost, C. and  
298 McGoon, D., 1971. A new reconstructive operation for correction of mitral and tricuspid insufficiency. The  
299 Journal of Thoracic and Cardiovascular Surgery, 61(1), pp.1-13. Available: 10.1016/s0022-5223(19)42269-  
300 1.
- 301
- 302 CME Exam for Guidelines for the Echocardiographic Assessment of the Right Heart in Adults: A  
303 Report from the American Society of Echocardiography. Journal of the American Society of  
304 Echocardiography, 23(7), pp. 786-788, 2010. Available: 10.1016/j.echo.2010.05.022.
- 305
- 306 Cohen, S., Sell, J., McIntosh, C. and Clark, R., 1987. Tricuspid regurgitation in patients with  
307 acquired, chronic, pure mitral regurgitation. The Journal of Thoracic and Cardiovascular Surgery, 94(4),  
308 pp.488-497. Available: 10.1016/s0022-5223(19)36208-7.
- 309
- 310 Dabiri, Y., Yao, J., Sack, K., Kassab, G. and Guccione, J., 2019. Tricuspid valve regurgitation  
311 decreases after mitraclip implantation: Fluid structure interaction simulation. Mechanics Research  
312 Communications, 97, pp.96-100. Available: 10.1016/j.mechrescom.2019.04.009.
- 313
- 314 David, T., David, C. and Manhiolt, C., 2015. When is tricuspid valve annuloplasty necessary  
315 during mitral valve surgery? The Journal of Thoracic and Cardiovascular Surgery, 150(5), pp.1043-1044.  
316 Available: 10.1016/j.jtcvs.2015.07.100.

- 317  
318 Dreyfus GD, Martin RP, Chan KM, Dulguerov F, Alexandrescu C., 2015. Functional tricuspid  
319 regurgitation: A need to revise our understanding. *Journal of the American College of Cardiology*, 65(21),  
320 pp.2331–2336. Available: <http://dx.doi.org/10.1016/j.jacc.2015.04.011>.
- 321  
322 Dwivedi, G., Mahadevan, G., Jimenez, D., Frenneaux, M. and Steeds, R., 2014. Reference values  
323 for mitral and tricuspid annular dimensions using two-dimensional echocardiography. *Echo Research  
324 and Practice*, 1(2), pp.43-50. Available: [10.1016/S0735-1097\(16\)32189-1](https://doi.org/10.1016/S0735-1097(16)32189-1).
- 325  
326 Fujimoto, N., Hastings, J., Bhella, P., Shibata, S., Gandhi, N., Carrick-Ranson, G., Palmer, D. and  
327 Levine, B., 2012. Effect of ageing on left ventricular compliance and distensibility in healthy sedentary  
328 humans. *The Journal of Physiology*, 590(8), pp.1871-1880. Available: [10.1113/jphysiol.2011.218271](https://doi.org/10.1113/jphysiol.2011.218271).
- 329  
330 Gaasch, W. and Meyer, T., 2008. Left Ventricular Response to Mitral Regurgitation. *Circulation*,  
331 118(22), pp.2298-2303. Available: [10.1161/circulationaha.107.755942](https://doi.org/10.1161/circulationaha.107.755942).
- 332  
333 Holzapfel, G. and Ogden, R., 2009. Constitutive modelling of passive myocardium: a structurally  
334 based framework for material characterization. *Philosophical Transactions of the Royal Society A:  
335 Mathematical, Physical and Engineering Sciences*, 367(1902), pp.3445-3475. Available:  
336 [10.1098/rsta.2009.0091](https://doi.org/10.1098/rsta.2009.0091).
- 337  
338 Huikuri, H., 1983. Effect of mitral valve replacement on left ventricular function in mitral  
339 regurgitation. *Heart*, 49(4), pp.328-333. Available: [10.1136/hrt.49.4.328](https://doi.org/10.1136/hrt.49.4.328).
- 340  
341 Izumi, J., Iga, K., and Konishi, T., 2002. Progression of isolated tricuspid regurgitation late after  
342 mitral valve surgery for rheumatic mitral valve disease. *Journal of Heart Valve Disease*, 11(03), pp. 353-  
343 356.
- 344  
345 Koelling, T., Aaronson, K., Cody, R., Bach, D. and Armstrong, W., 2002. Prognostic significance of  
346 mitral regurgitation and tricuspid regurgitation in patients with left ventricular systolic dysfunction.  
347 *American Heart Journal*, 144(3), pp.524-529. Available: [10.1067/mhj.2002.123575](https://doi.org/10.1067/mhj.2002.123575).
- 348  
349 Kong, F., Pham, T., Martin, C., McKay, R., Primiano, C., Hashim, S., Kodali, S. and Sun, W., 2018.  
350 Finite Element Analysis of Tricuspid Valve Deformation from Multi-slice Computed Tomography Images.  
351 *Annals of Biomedical Engineering*, 46(8), pp.1112-1127. Available: [10.1007/s10439-018-2024-8](https://doi.org/10.1007/s10439-018-2024-8).
- 352  
353 Kunzelman, K.S. and R. P. Cochran, R. P., 1990. Mechanical Properties of Basal and Marginal  
354 Mitral Valve Chordae Tendineae. *ASAIO Transactions*, 36(3), pp.M405-8.
- 355  
356 Le Huu, A. and Shum-Tim, D., 2014. Tissue engineering of autologous heart valves: a focused  
357 update. *Future Cardiology*, 10(1), pp.93-104. Available: [10.2217/fca.13.96](https://doi.org/10.2217/fca.13.96)
- 358  
359 Le Huu, A. and Shum-Tim, D., 2020. Transcatheter valve replacement: a revolution. *Future  
360 Cardiology*. Available: [10.2217/fca-2019-0011](https://doi.org/10.2217/fca-2019-0011)
- 361  
362 Lee, C., Laurence, D., Ross, C., Kramer, K., Babu, A., Johnson, E., Hsu, M., Aggarwal, A., Mir, A.,  
363 Burkhardt, H., Towner, R., Baumgart, R. and Wu, Y., 2019. Mechanics of the Tricuspid Valve—From  
364 Clinical Diagnosis/Treatment, In-Vivo and In-Vitro Investigations, to Patient-Specific Biomechanical  
365 Modeling. *Bioengineering*, 6(2), p.47. Available: [10.3390/bioengineering6020047](https://doi.org/10.3390/bioengineering6020047).

- 366  
367 May-Newman, K. and Yin, F., 1995. Biaxial mechanical behavior of excised porcine mitral valve  
368 leaflets. American Journal of Physiology-Heart and Circulatory Physiology, 269(4), pp.H1319-H1327.  
369 Available: [10.1152/ajpheart.1995.269.4.h1319](https://doi.org/10.1152/ajpheart.1995.269.4.h1319).
- 370  
371 Modin, D., Møgelvang, R., Andersen, D. and Biering- Sørensen, T., 2019. Right Ventricular  
372 Function Evaluated by Tricuspid Annular Plane Systolic Excursion Predicts Cardiovascular Death in the  
373 General Population, Journal of the American Heart Association, 8(10). Available:  
374 [10.1161/jaha.119.012197](https://doi.org/10.1161/jaha.119.012197).
- 375  
376 Morgan, A., Howell, K., Chen, S., Serrone, R., Zheng, Y., Wang, V., Kim, J., Grossi, E., Selzman,  
377 C., Guccione, J., Sharma, V., MacLeod, R. and Ratcliffe, M., 2020. Imaging and computational modeling  
378 of tricuspid regurgitation and repair. Vessel Plus, 4(6). Available: <https://doi.org/10.20517/2574-1209.2019.32>.
- 380  
381 Pfannmüller, B., Doenst, T., Eberhardt, K., Seeburger, J., Borger, M. and Mohr, F., 2012.  
382 Increased risk of dehiscence after tricuspid valve repair with rigid annuloplasty rings. The Journal of  
383 Thoracic and Cardiovascular Surgery, 143(5), pp.1050-1055. Available: [10.1016/j.jtcvs.2011.06.019](https://doi.org/10.1016/j.jtcvs.2011.06.019).
- 384  
385 Rahmani, S., Ebrahimi, B., Heidari, A., Navidbakhsh, M., Alizadeh, M. and Tafti, H., 2019.  
386 Hemodynamic investigation of subclavian-coronary steal syndrome in dialysis patients with coronary  
387 artery occlusion and different stenosis percentages in subclavian artery. Journal of Mechanics in Medicine  
388 and Biology, 19(06), p.1950052. Available: [10.1142/S0219519419500520](https://doi.org/10.1142/S0219519419500520)
- 390  
391 Sahli Costabal, F., Hurtado, D. and Kuhl, E., 2016. Generating Purkinje networks in the human  
392 heart. Journal of Biomechanics, 49(12), pp.2455-2465. Available: [10.1016/j.jbiomech.2015.12.025](https://doi.org/10.1016/j.jbiomech.2015.12.025).
- 393  
394 Sakamoto, Y., Buchanan, R., Sanchez-Adams, J., Guilak, F. and Sacks, M., 2017. On the  
395 Functional Role of Valve Interstitial Cell Stress Fibers: A Continuum Modeling Approach. Journal of  
396 Biomechanical Engineering, 139(2). Available: [10.1115/1.4035557](https://doi.org/10.1115/1.4035557)
- 397  
398 Shalaby, N., Zemzemi, N. and Elkhodary, K., 2019. Simulating the effect of sodium channel  
399 blockage on cardiac electromechanics. Proceedings of the Institution of Mechanical Engineers, Part H:  
400 Journal of Engineering in Medicine, 234(1), pp.16-27. Available: [10.1177/0954411919882514](https://doi.org/10.1177/0954411919882514)
- 401  
402 Shubaiber, J., 2018. Tricuspid valve annulus surgery during mitral valve surgery. Journal of  
403 Thoracic Disease, 10(6), pp.3156-3157. Available: [10.21037/jtd.2018.05.157](https://doi.org/10.21037/jtd.2018.05.157).
- 404  
405 Singh-Gryzbon, S., Sadri, V., Toma, M., Pierce, E., Wei, Z. and Yoganathan, A., 2019.  
406 Development of a Computational Method for Simulating Tricuspid Valve Dynamics. Annals of Biomedical  
407 Engineering, 47(6), pp.1422-1434. Available: [10.1007/s10439-019-02243-y](https://doi.org/10.1007/s10439-019-02243-y).
- 408  
409 Streeter, D., Spotnitz, H., Patel, D., Ross, J. and Sonnenblick, E., 1969. Fiber Orientation in the  
410 Canine Left Ventricle during Diastole and Systole. Circulation Research, 24(3), pp.339-347. Available:  
411 [10.1161/01.res.24.3.339](https://doi.org/10.1161/01.res.24.3.339).
- 412  
413 Verdonk, C., Darmon, A., Cimadevilla, C., Lepage, L., Raffoul, R., Nataf, P., Vahanian, A. and  
414 Messika-Zeitoun, D., 2018. Is tricuspid annuloplasty increasing surgical mortality and morbidity during  
mitral valve replacement? A single-centre experience. Archives of Cardiovascular Diseases, 111(8-9),

- 415 pp.480-486. Available: 10.1016/j.acvd.2017.08.006.
- 416
- 417 Walker, J., Ratcliffe, M., Zhang, P., Wallace, A., Fata, B., Hsu, E., Saloner, D. and Guccione, J.,  
418 2005. MRI-based finite-element analysis of left ventricular aneurysm. American Journal of Physiology-  
419 Heart and Circulatory Physiology, 289(2), pp.H692-H700. Available: 10.1152/ajpheart.01226.2004.
- 420
- 421 Weese, J., Smith, N., Razavi, R., Chapelle, D., Delingette, H., Frangi, A., Hose, R., Hunter, P. and  
422 Spaan, J., 2013. [online] Euheart.eu. Available at:  
423 <[http://www.euheart.eu/fileadmin/system/euheart/documents/euHeart\\_report.pdf](http://www.euheart.eu/fileadmin/system/euheart/documents/euHeart_report.pdf)> [Accessed 21 April  
424 2020].
- 425
- 426 Wei, J., Chang, C., Lee, F. and Lai, W., 1993. De Vega's semicircular annuloplasty for tricuspid  
427 valve regurgitation. The Annals of Thoracic Surgery, 55(2), pp.482-485. Available: 10.1016/0003-  
428 4975(93)91023-g.

# Patient-Specific Finite Element Analysis of Heart Failure: Mitral Valve Replacement and Tricuspid Valve Repair

Yousof M.A. ABDEL-RAOUF<sup>1</sup>, Alireza HEIDARI<sup>2,3\*</sup>, Khalil ELKHODARY<sup>1</sup>, Mohamed BADRAN<sup>4</sup>, Hojatollah VALI<sup>3</sup>, Masoud ASGHARIAN<sup>2</sup>, Antony A.YOUSSEF<sup>1</sup>, Cristina POP<sup>5</sup>, Dominique SHUM-TIM<sup>6</sup>

<sup>1</sup> Department of Mechanical Engineering, American University in Cairo, 11835, New Cairo, Egypt

<sup>2</sup> Department of Mathematics and Statistics, McGill University, Montreal, QC, H3A 0B9, Canada

<sup>3</sup> Department of Anatomy and cell biology, McGill University, Montreal, QC, H3A 0B9, Canada

<sup>4</sup>Mechanical Engineering Department, Future University in Egypt, 11835, New Cairo, Egypt

<sup>5</sup>Department of Medicine, Faculty of Medicine, McGill University. Montreal, Canada

<sup>6</sup>Department of Surgery, McGill University Health Center, Montreal, QC, H4A 3J1, Canada

\*Corresponding author. Email Address: alireza.heidari@mcgill.ca

Tel: + 1-514-962-2600; fax: +1-514-398-5047

Submitted: July 17, 2020

Word Count: 2888

**Keywords:** Mitral Valve Regurgitation, Tricuspid Valve Repair, Heart Failure, Annuloplasty Ring, Finite Element Analysis.

## Abstract

Tricuspid annuloplasty is often recommended to mitigate the possible onset of right-sided heart failure in patients presenting with annular dilatation or tricuspid valve regurgitation (TR). This is an underreported clinical issue, especially when tricuspid valve (TV) failure occurs following invasive and non-invasive interventions such as mitral valve replacement or commissurotomy. We present the case of a 72-year-old female patient with severe mitral valve regurgitation who underwent mitral valve replacement, and we demonstrate the computational model used to predict the necessity of a tricuspid annuloplasty in addressing the possible development of secondary tricuspid regurgitation. A full-heart electro-mechanical finite element model was used to simulate the patient's heart based on magnetic resonance imaging (MRI) images prior to surgery and 3 days following surgery. Comparison of patient geometry pre-operation and post-operation showed a change in shape of the TV in systole. A rigid constraint across the TV annulus (TA) was used to simulate an annuloplasty ring. The desirable increase in ring-widening forces is

34 predicted post-operation, with a significant reduction in contractile forces being exerted on the ring. Our  
35 model leads us to conclude that the patient will likely develop TV annular dilatation and subsequent  
36 regurgitation in the absence of further surgical intervention. We further highlight a general need to  
37 investigate by means of patient-specific in silico models valvular features in patients presenting with left-  
38 sided valvular disease, as computational modeling has greatly enhanced our ability to study their  
39 associated phenomena with more scrutiny and in real time. Such models have the potential to allow  
40 physicians better pre-surgical planning and prediction of short- and long-term patient outcomes.

41 **1. Introduction**

42 Mitral Valve Regurgitation (MR) is a valvular disease affecting approximately 0.59% of adults and with  
43 its prevalence increasing significantly with age (Dziadko and Enriquez-Sarano, 2016). MR is associated  
44 with Left Ventricular (LV) dysfunction, is characterized by incomplete Mitral Valve (MV) leaflet  
45 coaptation, and in severe cases leads to Heart Failure (HF). It is also a major factor in the onset of  
46 Pulmonary Hypertension (PH), creating a higher RV afterload, ultimately causing Right Ventricular (RV)  
47 dilation, Tricuspid annulus (TA) dilation and secondary Tricuspid Valve Regurgitation (TR) (Badano et  
48 al., 2013). This is also termed Functional TR (FTR) and occurs in approximately 30% to 50% of those with  
49 severe MR (Cohen et al., 1987; Koelling et al., 2002), with incidences of severe FTR in approximately 14%  
50 of patients who underwent MV replacement (Izumi et al., 2002).

51 While common for patients with severe MR to undergo MV replacement surgery, assessment of FTR  
52 and agreement on intervention and its necessity, in the form of TV annuloplasty varies among experts in  
53 the cardiologist community (David et al., 2015; Shuhaiber, 2018), with many drafting different guidelines  
54 to help classify patients and their respective intervention policies (Dreyfus et al., 2015; Verdonk et al.,  
55 2018). Many procedures regarding repair of the TV exist, including the suturing of two TV leaflets at the  
56 middle of their edges called the “clover” technique (Bellushi et al., 2018), and recently the adaptation of  
57 an intervention previously used to treat regurgitant MV leaflets by pinching them together using a device  
58 named MitralClip (Dabiri et al., 2019). On the other hand, the De Vega technique involves the suture of  
59 components of the TA (Wei et al., 1993), and the use of annuloplasty rings, first employed by (Carpentier  
60 et al., 1971), has become a popular choice for valve repair. Both rigid and semi-rigid rings can be used and

61 the choice between them will determine the amount of TA remodeling, although care must be given to the  
62 cardiac tissue's ability to withstand the large cyclical forces (Pfannmüller et al., 2012).

63 With the recent increase of computational tools, attention has been given to creating computational  
64 models of the heart that reflect anatomical and physiological diseases which lend insight into relevant  
65 pathophysiology, complications and intervention policies. For instance, (Shalaby et al., 2019) investigate  
66 computationally the complications that arise from drug cardiotoxicity, as reflected in distorted ECGs,  
67 altered cardiac function. Additionally, computational studies serve as a decision-making aid to questions  
68 where there is no established clinical consensus on assessment and intervention policies. Work by  
69 (Rahmani et al., 2019) leverages such tools in predicting the subclavian steal syndrome (SSS) occurrence  
70 in haemodialysis patients undergoing coronary artery bypass (CABG) by assessing the arterial stenosis.  
71 They were able to determine a threshold of stenosis at 54% beyond which retrograde flow in the  
72 subclavian artery would lead to the steal phenomenon and computational modelling was the only method  
73 to quantitatively investigate it. Previous work highlighting the effect of novel annuloplasty on regurgitant  
74 MV has been presented (Baillargeon et al., 2015). More recent work focused on Finite Element (FE) TV  
75 modelling and presents patient-specific dynamics of healthy TV geometry obtained using Multi-sliced  
76 computer tomography (MSCT), and a hyperelastic formulation for the material response (Kong et al.,  
77 2018). A subsequent analysis by (Singh-Gryzbon et al., 2019) addressed some of the assumptions made in  
78 (Kong et al., 2018) regarding chordae tendinea and papillary muscle locations, by setting up an  
79 experimental framework to capture TV-chordae geometry, while employing Fluid Structure Interaction  
80 (FSI) to computationally determine the effect of TR on hemodynamic. Most recently, (Dabiri et al., 2019)  
81 have used FSI to demonstrate the application of MitraClip, and its ability to reduce regurgitation in the  
82 TV. Highlighting the interplay between RV dynamics and the TV will greatly add to our understanding of  
83 the etiology and intervention policies pertaining to FTR, especially since FTR is a product of RV failure or  
84 remodelling (Lee et al., 2019; Morgan et al., 2019). To our knowledge that there has not been any full  
85 heart computational modelling which investigates this important issue.

86 To that end, we present herein the case of a 72-year-old female symptomatic with chest pain and  
87 exertional dyspnea, suffering severe MVR, PH and Left Atrial (LA) dilation. Based on the benefits that  
88 tissue-based valves afford patients (Le Huu and Shum-Tim, 2014), it was concluded that the patient  
89 would undergo MV replacement using a bioprosthetic valve. We present a simulation of the full patient

90 heart before and after surgery using the (FE) method in which we examine the ventricle-valve dynamics.  
91 We also simulate the presence of a TV annuloplasty ring to demonstrate that if annuloplasty is not  
92 undertaken it is predicted that the patient post MV-replacement surgery will nonetheless likely develop  
93 FTR and RV failure due to excessive cyclical forces on the annulus that lead to Tricuspid Annulus (TA)  
94 dilation.

95 **2. Methodology**

96 *2.1. Patient Specification*

97 A patient-specific geometry and corresponding cardiac function were obtained from a transthoracic  
98 echocardiogram (TTE) and cardiac magnetic resonance (CMR) (**Fig. 1**). The patient underwent  
99 bioprosthetic mitral valve replacement (Biologic Epic #29) (Abbott Laboratories, Chicago, IL, USA) and  
100 tricuspid valve repair (Ring #30) at Tehran Heart Center, Iran. While transcatheter deployment of the  
101 artificial valve presented a less invasive option (Le Huu and Shum-Tim, 2020), the patient underwent  
102 open-heart surgery due to tricuspid valve repair. Patient underwent surgical management as determined  
103 by the surgical team at the Tehran Heart Center as per the most recent guidelines. Patient-specific  
104 simulation using computational modeling was done in a prospective matter, such that imaging was  
105 performed, and medical records were obtained throughout the patient's management without interference  
106 with the pre-established treatment.

107 CMR imaging was acquired by multi-planar MR sequences using true fast imaging with steady state  
108 procession (truFISP), truFISP cine, whole heart coronary imaging, and 3D contrast-enhanced high-  
109 resolution MR angiography (MRA) of the vessels of the chest and upper abdomen with administration of  
110 20 ml of Gadolinium contrast agent.

111 *2.2. Simulation*

112 We begin with an initial geometry, i.e. an idealized 3D CAD heart model (Zygote Media Group Inc.,  
113 American Fork, UT, USA). We modified this initial geometry by adopting a dilation-based morphing  
114 method and reshaped the cardiac chambers into the dilated states which corresponded to patient geometry  
115 (Athanasios, 2019). Heart remodeling before and after surgery was thus simulated.

116 The network of Purkinje fibers corresponding to our patient is composed of 3D truss elements, in a  
117 fractal pattern, spanning the endocardium (Sahli et al., 2016). In order to morph these fibers according to

118 patient's ventricular geometries, a zero-distance mapping constraint described in Eqn. 1 was enforced  
 119 between Purkinje nodes and ventricular nodes.

120  $P(x,y,z) - N(x,y,z) = P'(x,y,z) - N'(x,y,z)$ , (1)

121 Where  $P(x,y,z)$  and  $P'(x,y,z)$  correspond to the initial Purkinje fiber nodal coordinates and morphed  
 122 coordinates respectively, and  $N(x,y,z)$  and  $N'(x,y,z)$  correspond to the nearest initial ventricular nodal  
 123 coordinates and morphed nodal coordinates respectively. A schematic of the adjustment methodology is  
 124 shown in **Fig. 2**.

125 We further simulated for three cardiac cycles the mechanical response of the remodeled geometries on  
 126 the Living Heart Human Model (LHHM) in Abaqus 2019 (Baillargeon et al., 2014). In the LHHM, the  
 127 atria and ventricles have been discretized into 263,028 3D deformable linear tetrahedral elements.  
 128 Ventricular fiber orientations are applied to element centroids in accordance to the method of (Streeter et  
 129 al., 1969), while atrial fiber orientations are assigned in correspondence to the findings of the euroHeart  
 130 project (Weese et al., 2007).

131 The passive response of the chambers is modeled as incompressible, anisotropic, and hyperelastic, as  
 132 given by the Strain Energy Function (Holzapfel and Ogden, 2009):

133  $\Psi_{deviatoric} = \frac{a}{2b} e^{b(I_1 - 3)} + \sum_{i=f,s} \frac{a_i}{2b_i} (e^{b_i(I_{4i} - 1)^2} - 1) + \frac{a_{fs}}{2b_{fs}} (e^{b_{fs}(I_{8fs})^2} - 1)$ , (2)

134  $\Psi_{volumetric} = \frac{1}{D} \left( \frac{J^2 - 1}{2} - \ln(J) \right)$ , (3)

135 Where  $a$ ,  $b$ ,  $a_f$ ,  $a_s$ ,  $a_{fs}$  and  $b_{fs}$  are material constants. The value of  $I_1$  describes the isotropic response and  
 136 is the first principal invariant of the left Cauchy-Green tensor,  $\mathbf{C}$ , and is given by  $I_1 = \text{tr}(\mathbf{C})$ . The two  
 137 invariants that describe transversely isotropic behavior are  $I_{4f}$ ,  $I_{4s}$ , each being evaluated as  $\mathbf{f}_o \cdot (\mathbf{C} \mathbf{f}_o)$  and  
 138  $\mathbf{s}_o \cdot (\mathbf{C} \mathbf{s}_o)$  respectively. Finally, the orthotropic response is incorporated in the term  $I_{8fs} = \mathbf{f}_o \cdot (\mathbf{C} \mathbf{s}_o)$ . The  
 139 directions  $\mathbf{f}$  and  $\mathbf{s}$  are evaluated at any time as  $\mathbf{F} \mathbf{f}_o$  and  $\mathbf{F} \mathbf{s}_o$  where  $\mathbf{F}$ ,  $\mathbf{f}_o$  and  $\mathbf{s}_o$  are the deformation  
 140 gradient, fiber direction and sheet direction respectively. The volumetric response is composed of the bulk  
 141 modulus,  $D$ , and the Jacobian,  $J$ .

142 Conversely, an active material response reflecting the electrically sensitive tension along the myofibers,  
 143 as given by Walker et al. (Walker et al., 2004), is adopted:

144  $\sigma(t, E_{ff})_{\text{active fiber}} = T_{\max} \frac{C_{a_0}^2}{2(C_{a_0}^2 + EC_{a_50}^2)} (1 - \cos(\omega))$ , (4a)

145  $ECa_{50} = \frac{Ca_0 \max}{\sqrt{e^{B(l-l_0)} - 1}},$  (4b)

146  $\omega = \begin{cases} \pi \frac{t}{t_0}, & \text{when } 0 \leq t \leq t_0 \\ \pi \frac{t-t_0+t_r}{t_r}, & \text{when } t_0 \leq t \leq t_0 + t_r \\ 0, & \text{when } t_0 + t_r \leq t \end{cases}$

147 (4c)

148  $t_r = ml + b,$  (4d)

149  $l = l_r \sqrt{2E_{ff} + 1},$  (4e)

150 Where  $T_{max}$  is the maximum active stress in the fiber,  $Ca_o$  and  $Ca_{omax}$  represent peak Calcium  
 151 concentration in the myofiber,  $l_o$  is the minimum sarcomere length at which active stress develops,  $l_o$  is  
 152 the initial fiber length,  $t_o$  is the time until maximum stress is reached,  $B$ ,  $m$  and  $b$  are phenomenological  
 153 constants and finally,  $E_{ff}$  is the Green-Lagrange strain component along the fiber direction.

154 The true stress along the fiber will therefore be

155  $\sigma_{fiber} = \sigma_{passive\ fiber} + \sigma_{active\ fiber},$  (5)

156 Fine tuning the aforementioned parameters was a necessary step to obtain the appropriate patient-  
 157 specific Ejection Fraction (EF) and to reflect the increase in stiffness associated with ageing described in  
 158 literature (Walker et al., 2005; Fujimoto et al., 2012).

### 159 2.3. FTR and Annuloplasty

160 The TV and MV were discretized into denser meshes of 21,252 and 70,210 deformable 3D linear  
 161 tetrahedral elements respectively. Chordae were modeled as truss elements and chordae-TV interactions  
 162 and TV-RV interactions were defined by distributed coupling, and the chordae were fixed to the Papillary  
 163 Muscles (PM) using a tie-constraint (Abaqus Analysis User's Manual, 2014). The material constants used  
 164 in this work to describe the MV and TV have been also adjusted to represent the stresses described in  
 165 May-Newman and Yin (May-Neumann and Yin, 1995). Chordae and PM location have been adjusted to  
 166 simulate complete closure in the neutral RV geometry. The TA in our model is defined as the region of the  
 167 ventricles to which the valves are attached. Local fiber orientations of the valve and corresponding biaxial  
 168 data describing the isotropic Marlow hyperelastic material response of the chordae were adapted from  
 169 (Kunzleman and Cochran, 1990). It is also important to note that previous work has commented on the

170 mechanics of valve interstitial cells (VICs) which undergo unique viscoelastic dynamics (Sakamoto et al.,  
171 2017), and this has been overlooked in this work for simplicity. A 0D-Windkessel model was used to  
172 extract fluid pressure across the different cardiac chambers, and patient-specific transvalvular pressure  
173 was thus applied to the ventricular sides of the TV leaflets.

174 To model the post-operative geometry for the patient, their MV geometry must be forgone (due to the  
175 replacement). We instead model the effect of the replacement valve and ring using connector elements.  
176 This is done by constraining 20 nodes which substitute for suture points between the new ring/valve  
177 complex and the ventricles (Baillargeon et al., 2015). Each node is connected to its neighbor by a rigid link  
178 in a circumferential formation (**Fig. 3**) to remove relative motion between suture points, and to mimic the  
179 mechanical effect of the new ring/MV complex (Abaqus Analysis User's Manual, 2014).

180 Surgical intervention planning for TV repair requires a thorough understanding of the state of the TA. In  
181 order to study the behavior of the TA pre- and post-operatively, we further define a hypothetical ring as  
182 above for the TA, so that forces measured along the ring would directly reflect TA dynamics in the cardiac  
183 cycle. We assign wire connector elements that link 40 ventricular nodes along the TA, using rigid links to  
184 constrain their relative motion and to simulate the effect of a rigid annuloplasty ring. Average link length  
185 was  $3.74 \pm 1.22$  mm in the pre-operative geometry and  $4.07 \pm 2.44$  mm in the post-operative geometry.

186 We also explore the effect of using rigid and semi-rigid links on the forces in the TA for the post-operative  
187 geometry. In the semi-rigid case, axial connectors are prescribed an elasticity and a damping, as  
188 characteristic of the behavior of a spring-dashpot (Abaqus Analysis User's Manual, 2014). Resulting forces  
189 on these elements are compared to help elucidate the difference between forces on the TA before MV  
190 replacement and after.

### 191 **3. Results**

192 Pre-operatively, echocardiography and magnetic resonance imaging showed for the patient biatrial  
193 enlargement, while RV and LV size were within normal range. Velocity flow assessment showed severe  
194 mitral regurgitation, thickened leaflets, mild mitral stenosis (mitral valve area =  $1.8 \text{ cm}^2$ , mean gradient 5  
195 mmHg), and echocardiography showed Pulmonary arterial pressure was 70 mmHg, compared to 64  
196 mmHg upon right heart catheterization.

197 Following mitral valve replacement and tricuspid valve repair, a CMR was repeated for the patient.  
198 There was an estimated 15% reduction in LA, resulting in a 30% reduction in LA cavity volume, while the  
199 RA remained normal in size. Velocity flow mappings showed no mitral regurgitation, with a mild tricuspid  
200 regurgitation. There was a significant reduction in pulmonary hypertension to 30 mmHg on repeat TTE.  
201 There was persistent global LV and RV hypokinesis, which is compatible with chronic cardiac remodeling  
202 as seen with non-ischemic dilated cardiomyopathy (Huikiri, 1983; Gaasch and Meyer, 2008).

203 Dilated pre-operative patient volume and shape were simulated in our model, and an atrial view of the  
204 valves shows severe MR mid-systole (**Fig. 4**). We also simulated a reduced Tricuspid Annular Systolic  
205 Excursion (TAPSE), reporting a value of 13.78 mm. End diastolic (ED) TA diameter calculated from the  
206 septal segment to the lateral segment was  $46.24 \pm 5.26$  mm. Maximum principle stress was largest at the  
207 MV - aortic root, and maximum principle strain is largest at TV and MV leaflet bellies, with the largest  
208 strain being located in the Anterior Tricuspid Leaflet (ATL) compared to the other TV leaflets (**Fig. 5a,c**).

209 Modeled post-operative geometry also showed the remodeled TA to be more rounded, and that the ED  
210 TA annulus was reduced slightly to  $44.06 \pm 1.11$  mm. The replaced MV has noticeably decreased stress at  
211 the aortic root (**Fig. 5b**), as well as increased strain distribution across TV leaflets (**Fig. 5d**).

212 A comparison of the forces exerted by the TA showed post-operative TA to have a mildly higher force  
213 (~2 N) in diastole while pre-operative TA exhibited a remarkably larger force during the systolic phase (~  
214 42 N) (**Fig. 6**). The segments of TA experiencing the highest forces in the pre-operative geometry were  
215 located at the antero-lateral segment of the TA with a peak average force of  $2.990 \pm 0.038$  N, while post-  
216 operative geometry experiences the highest forces at the septal region with a peak average force of  $1.144 \pm$   
217 0.020 N (**Fig. 7**).

218 After ascribing a spring-dashpot axial behavior to the links on the post-operative geometry, a  
219 significant reduction in total force was observed on contraction (**Fig. 8**). A breakdown of TA forces is  
220 shown in **Table 1**.

221 **Table 1** Breakdown of Total Forces on Pre-Operative and Post-Operative Geometries.

	Constraint Type	Max. (N)	Min. (N)	Average (N)
Pre-Operative	Rigid	65.54	1.38	12.05
	Rigid	21.67	3.06	7.50
Post-Operative	Semi-Rigid	17.39	2.77	6.48

222    **4. Discussion**

223    In this prospective study, we highlight the role of native geometry of the ventricles on valve dynamics.  
224    This is important to reflect valve diseases that do not result from leaflet abnormality but rather changes in  
225    the valve-chordae-ventricle complex. Patient geometry was replicated and TAPSE indicated reduced RV  
226    function and imminent RV failure (CME Exam for Guidelines, 2010; Modin et al., 2019). LA dilation in  
227    pre-operative geometry was the main cause of MVR in our model, demonstrating an accurate portrayal of  
228    left-side failure by our model. Additionally, RA dilation pre-operatively, and its size reduction post-  
229    operatively, created a TV diameter > 40 mm, which indicates the need for TV repair (Dreyfus et al., 2015;  
230    Verdonk et al., 2018). We herein report TV stresses and stress distributions in agreement with Kong et. al.  
231    (2018) and Singh-Gryzbon et al. (2019).

232    Analysis of the forces on TA suggest that during the cardiac cycle TA widening post operatively was  
233    larger, indicating that over time the TA would dilate. Moreover, TA contraction was shown to be  
234    significantly reduced post-operatively, indicating valve closure would be impaired with time. This, along  
235    with the enlarged TA diameter and the patient's MV replacement suggest the patient now presents the key  
236    markers for which the ACA/AHA guidelines recommend TV repair (ACC/AHA 2006 Guidelines, 2006).

237    In the comparison of rigid and semirigid rings, our model demonstrated notably larger forces on rigid  
238    constraints, which suggests a more likely failure mode in accordance with clinical findings (Pfannmüller  
239    et al., 2012). Hence, it seems advisable that a full description of the mechanical properties of ring  
240    material, be incorporated in the *in-silico* model, is necessary for further detail of the behavior of a selected  
241    annuloplasty ring during pre-operative planning.

242    Employing an idealized shape of the TV and MV instead of segmentation is a clear limitation of our  
243    approach in this manuscript; however, our focus is not to study valve behavior alone, but rather the  
244    behavior of the ventricle-valve-chordae complex, rendering our simplification an important expedience.  
245    Furthermore, the mechanical description of the TA in our model is also simplified, not taking into account  
246    the tiered nature of the TA which transitions from a cardiomyocyte-dominant tissue to a cell-free  
247    collagenous tissue. Lastly, our use of 40 nodes to corresponding to 40 sutures was not patient-specific, an  
248    assumption which affects the exact magnitudes of forces reported on the TA.

249     **5. Conclusion**

250         A computational model for the human heart is geometrically and functionally adapted to simulate  
251         a patient-specific heart, using magnetic resonance images before and three days after surgery. Our study  
252         demonstrates a computational method that can be turned into a decision-making support tool for medical  
253         practitioners to use with FTR and TV repair. We have shown our computational approach is capable of  
254         predicting TV failure following surgical procedures on the left side of the heart for Mitral Valve  
255         Replacement. Our approach can quantitatively study several scenarios for TV repair using ring  
256         annuloplasty, giving insight into forces and stresses that can be invaluable to the pursuit of better  
257         understanding of valve repair and its efficiency.

258     **Conflict of interest**

259         The authors wish to declare no conflict of interest.

260     **Acknowledgements**

261         YA wishes to gratefully acknowledge the support of the Al-Alfi Foundation through the AL-Alfi  
262         Graduate Studies Fellowship. AH would like to express his gratitude to the Iranian Elite Foundation and  
263         Tehran Heart Centre for their support at the early stages of this project as well as Dr. Sara Sheibani at  
264         McGill department of Anatomy and Cell Biology for technical support related to the physiological  
265         parameters in the model. MA's research is partly supported by NSERC Canada. The authors are grateful  
266         for the invaluable help and collaboration of the members of the Living Heart Project and their research  
267         team.

268

269 **References**

- 270 Abaqus Analysis User's manual, Dassault Systèmes, Simulia Corp. Version 6.14., Providence, RI,  
271 2014 .
- 272
- 273 ACC/AHA 2006 Guidelines for the Management of Patients with Valvular Heart Disease:  
274 Executive Summary. Circulation, 114(5), pp. 450-527, 2006. Available:10.1161/circulationaha.106.177303.
- 275
- 276 Athanasios, A., 2019. A computational model for dilated cardiomyopathy: morphology and  
277 electromechanics. M.Sc., Thesis, The American University in Cairo. Digital Archive and Research  
278 Repository (DAR).
- 279
- 280 Badano, L., Muraru, D. and Enriquez-Sarano, M., 2013. Assessment of functional tricuspid  
281 regurgitation. European Heart Journal, 34(25), pp.1875-1885. Available: 10.1093/eurheartj/ehs474.
- 282
- 283 Baillargeon, B., Rebelo, N., Fox, D., Taylor, R. and E. Kuhl, E., 2014. The Living Heart Project: A  
284 robust and integrative simulator for human heart function. European Journal of Mechanics - A/Solids,  
285 48, pp. 38-47. Available: 10.1016/j.euromechsol.2014.04.001.
- 286
- 287 Baillargeon, B., Costa, I., Leach, J., Lee, L., Genet, M., Toutain, A., Wenk, J., Rausch, M., Rebelo,  
288 N., Acevedo-Bolton, G., Kuhl, E., Navia, J. and Guccione, J., 2015. Human Cardiac Function Simulator for  
289 the Optimal Design of a Novel Annuloplasty Ring with a Sub-valvular Element for Correction of Ischemic  
290 Mitral Regurgitation. Cardiovascular Engineering and Technology, 6(2), pp.105-116. Available:  
291 10.1007/s13239-015-0216-z.
- 292
- 293 Belluschi, I., Del Forno, B., Lapenna, E., Nisi, T., Iaci, G., Ferrara, D., Castiglioni, A., Alfieri, O.  
294 and De Bonis, M., 2018. Surgical Techniques for Tricuspid Valve Disease. Frontiers in Cardiovascular  
295 Medicine, 5. Available: 10.3389/fcvm.2018.00118.
- 296
- 297 Carpenter, A., Deloche, A., Dauptain, J., Soyer, R., Blondeau, P., Piwnica, A., Dubost, C. and  
298 McGoon, D., 1971. A new reconstructive operation for correction of mitral and tricuspid insufficiency. The  
299 Journal of Thoracic and Cardiovascular Surgery, 61(1), pp.1-13. Available: 10.1016/s0022-5223(19)42269-  
300 1.
- 301
- 302 CME Exam for Guidelines for the Echocardiographic Assessment of the Right Heart in Adults: A  
303 Report from the American Society of Echocardiography. Journal of the American Society of  
304 Echocardiography, 23(7), pp. 786-788, 2010. Available: 10.1016/j.echo.2010.05.022.
- 305
- 306 Cohen, S., Sell, J., McIntosh, C. and Clark, R., 1987. Tricuspid regurgitation in patients with  
307 acquired, chronic, pure mitral regurgitation. The Journal of Thoracic and Cardiovascular Surgery, 94(4),  
308 pp.488-497. Available: 10.1016/s0022-5223(19)36208-7.
- 309
- 310 Dabiri, Y., Yao, J., Sack, K., Kassab, G. and Guccione, J., 2019. Tricuspid valve regurgitation  
311 decreases after mitraclip implantation: Fluid structure interaction simulation. Mechanics Research  
312 Communications, 97, pp.96-100. Available: 10.1016/j.mechrescom.2019.04.009.
- 313
- 314 David, T., David, C. and Manhiolt, C., 2015. When is tricuspid valve annuloplasty necessary  
315 during mitral valve surgery? The Journal of Thoracic and Cardiovascular Surgery, 150(5), pp.1043-1044.  
316 Available: 10.1016/j.jtcvs.2015.07.100.

- 317  
318 Dreyfus GD, Martin RP, Chan KM, Dulguerov F, Alexandrescu C., 2015. Functional tricuspid  
319 regurgitation: A need to revise our understanding. *Journal of the American College of Cardiology*, 65(21),  
320 pp.2331–2336. Available: <http://dx.doi.org/10.1016/j.jacc.2015.04.011>.
- 321  
322 Dwivedi, G., Mahadevan, G., Jimenez, D., Frenneaux, M. and Steeds, R., 2014. Reference values  
323 for mitral and tricuspid annular dimensions using two-dimensional echocardiography. *Echo Research  
324 and Practice*, 1(2), pp.43-50. Available: [10.1016/S0735-1097\(16\)32189-1](https://doi.org/10.1016/S0735-1097(16)32189-1).
- 325  
326 Fujimoto, N., Hastings, J., Bhella, P., Shibata, S., Gandhi, N., Carrick-Ranson, G., Palmer, D. and  
327 Levine, B., 2012. Effect of ageing on left ventricular compliance and distensibility in healthy sedentary  
328 humans. *The Journal of Physiology*, 590(8), pp.1871-1880. Available: [10.1113/jphysiol.2011.218271](https://doi.org/10.1113/jphysiol.2011.218271).
- 329  
330 Gaasch, W. and Meyer, T., 2008. Left Ventricular Response to Mitral Regurgitation. *Circulation*,  
331 118(22), pp.2298-2303. Available: [10.1161/circulationaha.107.755942](https://doi.org/10.1161/circulationaha.107.755942).
- 332  
333 Holzapfel, G. and Ogden, R., 2009. Constitutive modelling of passive myocardium: a structurally  
334 based framework for material characterization. *Philosophical Transactions of the Royal Society A:  
335 Mathematical, Physical and Engineering Sciences*, 367(1902), pp.3445-3475. Available:  
336 [10.1098/rsta.2009.0091](https://doi.org/10.1098/rsta.2009.0091).
- 337  
338 Huikuri, H., 1983. Effect of mitral valve replacement on left ventricular function in mitral  
339 regurgitation. *Heart*, 49(4), pp.328-333. Available: [10.1136/hrt.49.4.328](https://doi.org/10.1136/hrt.49.4.328).
- 340  
341 Izumi, J., Iga, K., and Konishi, T., 2002. Progression of isolated tricuspid regurgitation late after  
342 mitral valve surgery for rheumatic mitral valve disease. *Journal of Heart Valve Disease*, 11(03), pp. 353-  
343 356.
- 344  
345 Koelling, T., Aaronson, K., Cody, R., Bach, D. and Armstrong, W., 2002. Prognostic significance of  
346 mitral regurgitation and tricuspid regurgitation in patients with left ventricular systolic dysfunction.  
347 *American Heart Journal*, 144(3), pp.524-529. Available: [10.1067/mhj.2002.123575](https://doi.org/10.1067/mhj.2002.123575).
- 348  
349 Kong, F., Pham, T., Martin, C., McKay, R., Primiano, C., Hashim, S., Kodali, S. and Sun, W., 2018.  
350 Finite Element Analysis of Tricuspid Valve Deformation from Multi-slice Computed Tomography Images.  
351 *Annals of Biomedical Engineering*, 46(8), pp.1112-1127. Available: [10.1007/s10439-018-2024-8](https://doi.org/10.1007/s10439-018-2024-8).
- 352  
353 Kunzelman, K.S. and R. P. Cochran, R. P., 1990. Mechanical Properties of Basal and Marginal  
354 Mitral Valve Chordae Tendineae. *ASAIO Transactions*, 36(3), pp.M405-8.
- 355  
356 Le Huu, A. and Shum-Tim, D., 2014. Tissue engineering of autologous heart valves: a focused  
357 update. *Future Cardiology*, 10(1), pp.93-104. Available: [10.2217/fca.13.96](https://doi.org/10.2217/fca.13.96)
- 358  
359 Le Huu, A. and Shum-Tim, D., 2020. Transcatheter valve replacement: a revolution. *Future  
360 Cardiology*. Available: [10.2217/fca-2019-0011](https://doi.org/10.2217/fca-2019-0011)
- 361  
362 Lee, C., Laurence, D., Ross, C., Kramer, K., Babu, A., Johnson, E., Hsu, M., Aggarwal, A., Mir, A.,  
363 Burkhardt, H., Towner, R., Baumgart, R. and Wu, Y., 2019. Mechanics of the Tricuspid Valve—From  
364 Clinical Diagnosis/Treatment, In-Vivo and In-Vitro Investigations, to Patient-Specific Biomechanical  
365 Modeling. *Bioengineering*, 6(2), p.47. Available: [10.3390/bioengineering6020047](https://doi.org/10.3390/bioengineering6020047).

- 366  
367 May-Newman, K. and Yin, F., 1995. Biaxial mechanical behavior of excised porcine mitral valve  
368 leaflets. American Journal of Physiology-Heart and Circulatory Physiology, 269(4), pp.H1319-H1327.  
369 Available: 10.1152/ajpheart.1995.269.4.h1319.
- 370  
371 Modin, D., Møgelvang, R., Andersen, D. and Biering-Sørensen, T., 2019. Right Ventricular  
372 Function Evaluated by Tricuspid Annular Plane Systolic Excursion Predicts Cardiovascular Death in the  
373 General Population, Journal of the American Heart Association, 8(10). Available:  
374 10.1161/jaha.119.012197.
- 375  
376 Morgan, A., Howell, K., Chen, S., Serrone, R., Zheng, Y., Wang, V., Kim, J., Grossi, E., Selzman,  
377 C., Guccione, J., Sharma, V., MacLeod, R. and Ratcliffe, M., 2020. Imaging and computational modeling  
378 of tricuspid regurgitation and repair. Vessel Plus, 4(6). Available: <https://doi.org/10.20517/2574-1209.2019.32>.
- 380  
381 Pfannmüller, B., Doenst, T., Eberhardt, K., Seeburger, J., Borger, M. and Mohr, F., 2012.  
382 Increased risk of dehiscence after tricuspid valve repair with rigid annuloplasty rings. The Journal of  
383 Thoracic and Cardiovascular Surgery, 143(5), pp.1050-1055. Available: 10.1016/j.jtcvs.2011.06.019.
- 384  
385 Rahmani, S., Ebrahimi, B., Heidari, A., Navidbakhsh, M., Alizadeh, M. and Tafti, H., 2019.  
386 Hemodynamic investigation of subclavian-coronary steal syndrome in dialysis patients with coronary  
387 artery occlusion and different stenosis percentages in subclavian artery. Journal of Mechanics in Medicine  
388 and Biology, 19(06), p.1950052. Available: 10.1142/S0219519419500520
- 389  
390 Sahli Costabal, F., Hurtado, D. and Kuhl, E., 2016. Generating Purkinje networks in the human  
391 heart. Journal of Biomechanics, 49(12), pp.2455-2465. Available: 10.1016/j.jbiomech.2015.12.025.
- 392  
393 Sakamoto, Y., Buchanan, R., Sanchez-Adams, J., Guilak, F. and Sacks, M., 2017. On the  
394 Functional Role of Valve Interstitial Cell Stress Fibers: A Continuum Modeling Approach. Journal of  
395 Biomechanical Engineering, 139(2). Available: 10.1115/1.4035557
- 396  
397 Shalaby, N., Zemzemi, N. and Elkhodary, K., 2019. Simulating the effect of sodium channel  
398 blockage on cardiac electromechanics. Proceedings of the Institution of Mechanical Engineers, Part H:  
399 Journal of Engineering in Medicine, 234(1), pp.16-27. Available: 10.1177/0954411919882514
- 400  
401 Shubaiber, J., 2018. Tricuspid valve annulus surgery during mitral valve surgery. Journal of  
402 Thoracic Disease, 10(6), pp.3156-3157. Available: 10.21037/jtd.2018.05.157.
- 403  
404 Singh-Gryzbon, S., Sadri, V., Toma, M., Pierce, E., Wei, Z. and Yoganathan, A., 2019.  
405 Development of a Computational Method for Simulating Tricuspid Valve Dynamics. Annals of Biomedical  
406 Engineering, 47(6), pp.1422-1434. Available: 10.1007/s10439-019-02243-y.
- 407  
408 Streeter, D., Spotnitz, H., Patel, D., Ross, J. and Sonnenblick, E., 1969. Fiber Orientation in the  
409 Canine Left Ventricle during Diastole and Systole. Circulation Research, 24(3), pp.339-347. Available:  
410 10.1161/01.res.24.3.339.
- 411  
412 Verdonk, C., Darmon, A., Cimadevilla, C., Lepage, L., Raffoul, R., Nataf, P., Vahanian, A. and  
413 Messika-Zeitoun, D., 2018. Is tricuspid annuloplasty increasing surgical mortality and morbidity during  
414 mitral valve replacement? A single-centre experience. Archives of Cardiovascular Diseases, 111(8-9),

- 415 pp.480-486. Available: 10.1016/j.acvd.2017.08.006.
- 416
- 417 Walker, J., Ratcliffe, M., Zhang, P., Wallace, A., Fata, B., Hsu, E., Saloner, D. and Guccione, J.,  
418 2005. MRI-based finite-element analysis of left ventricular aneurysm. American Journal of Physiology-  
419 Heart and Circulatory Physiology, 289(2), pp.H692-H700. Available: 10.1152/ajpheart.01226.2004.
- 420
- 421 Weese, J., Smith, N., Razavi, R., Chapelle, D., Delingette, H., Frangi, A., Hose, R., Hunter, P. and  
422 Spaan, J., 2013. [online] Euheart.eu. Available at:  
423 <[http://www.euheart.eu/fileadmin/system/euheart/documents/euHeart\\_report.pdf](http://www.euheart.eu/fileadmin/system/euheart/documents/euHeart_report.pdf)> [Accessed 21 April  
424 2020].
- 425
- 426 Wei, J., Chang, C., Lee, F. and Lai, W., 1993. De Vega's semicircular annuloplasty for tricuspid  
427 valve regurgitation. The Annals of Thoracic Surgery, 55(2), pp.482-485. Available: 10.1016/0003-  
428 4975(93)91023-g.

## Figure Legends:

**Fig. 1** Echocardiography 4 chamber view of patient geometry pre-operation (a), pre-operation 3D patient model showing the four cardiac chambers (RA, RV, LA, LV) (b), CMR images of the 4 chamber-view (c), and Left side (d). White arrow in (a) indicates the widened MV annulus.

**Fig. 2** Illustration of Purkinje fibers (blue) reconstruction overlaid on-top of the two-chamber slice of the ventricles (grey). Ventricles are morphed, zero distance is kept between ventricular geometry and Purkinje fiber geometry.

**Fig. 3** Atrial view of the End Diastolic (ED) LV (red) corresponding to the post-operative geometry. The replaced MV geometry is not modelled, and the effects of this new MV are replicated using a rigid ring (white). The LA is not shown for clarity.

**Fig. 4** Atrial view of the mid-systolic biventricular pre-operative geometry. Meshing of the ventricles, valves and chordae were demonstrated as well as patient's incomplete coaptation of the MV. RA and LA geometries were removed for clarity.

**Fig. 5** Mid-systolic stress (a,b) and strain (c,d) distribution in TV, MV and ventricles in pre-operation and post-operation. The replacement of the MV with an annuloplasty ring shows a clear reduction in stress and strain at the Mitral Annulus (MA).

**Fig. 6** Comparison of forces on the TA shows a higher diastolic force post-operatively suggesting TA dilation is more likely. Reduced force during systole also suggests a loss of the role of the TA in coaptation

**Fig. 7** The location of the TA sections exhibiting the largest forces in pre-operative and post-operative geometries. (white).

**Fig. 8** A graph of total forces on rigid and semi-rigid rings shows a reduction of forces during the contraction, reflecting a reduced likelihood of dehiscence – or suture would trauma.

## Figures:

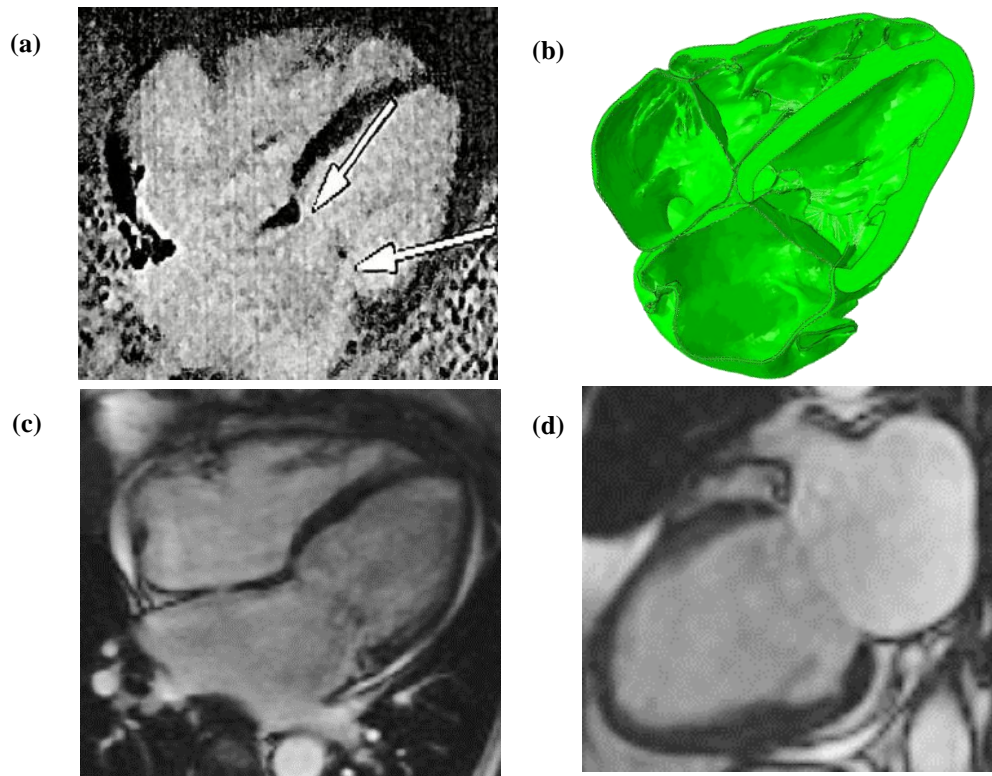


**Fig. 1** Echocardiography 4 chamber view of patient geometry pre-operation (a), pre-operation 3D patient model showing the four cardiac chambers (RA, RV, LA, LV) (b), CMR images of the 4 chamber-view (c), and Left side (d). White arrow in (a) indicates the widened MV annulus.

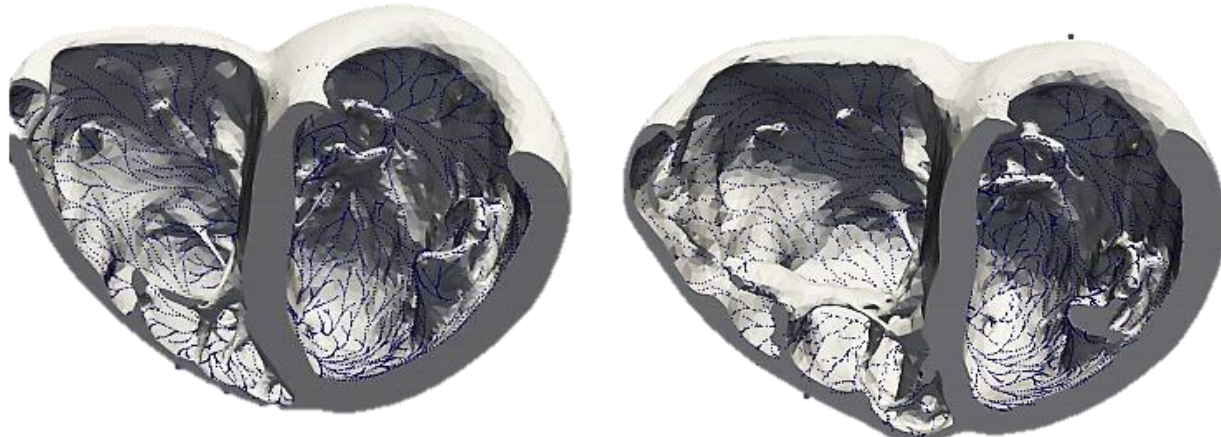


**Fig. 2** Illustration of Purkinje fibers (blue) reconstruction overlaid on-top of the two-chamber slice of the ventricles (grey). Ventricles are morphed, zero distance is kept between ventricular geometry and Purkinje fiber geometry.



**Fig. 3** Atrial view of the End Diastolic (ED) LV (red) corresponding to the post-operative geometry. The replaced MV geometry is not modelled, and the effects of this new MV are replicated using a rigid ring (white). The LA is not shown for clarity.

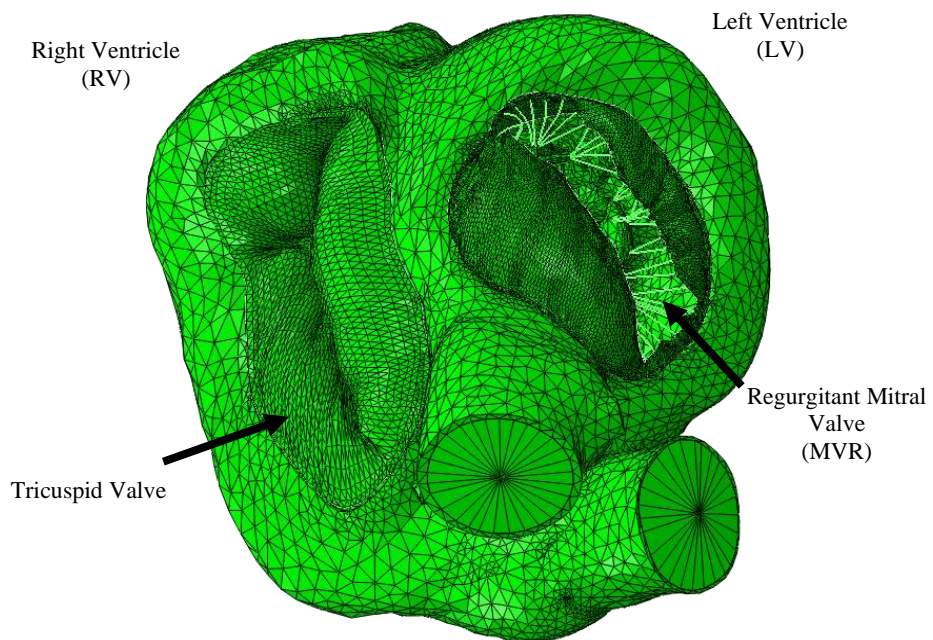


**Fig. 4** Atrial view of the mid-systolic biventricular pre-operative geometry. Meshing of the ventricles, valves and chordae were demonstrated as well as patient's incomplete coaptation of the MV. RA and LA geometries were removed for clarity.

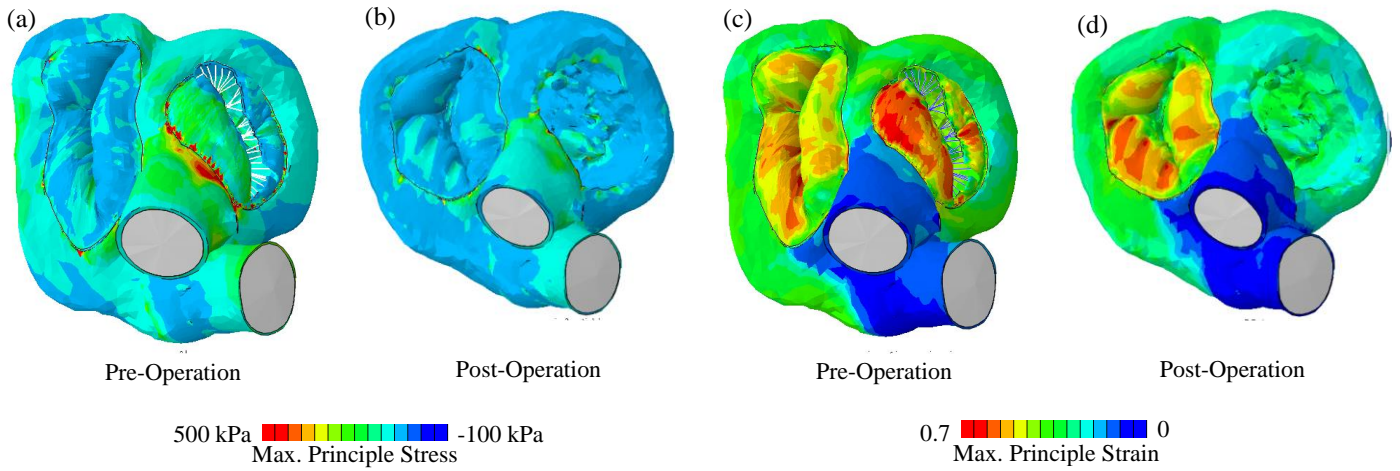


**Fig. 5** Mid-systolic stress (a,b) and strain (c,d) distribution in TV, MV and ventricles in pre-operation and post-operation. The replacement of the MV with an annuloplasty ring shows a clear reduction in stress and strain at the Mitral Annulus (MA).

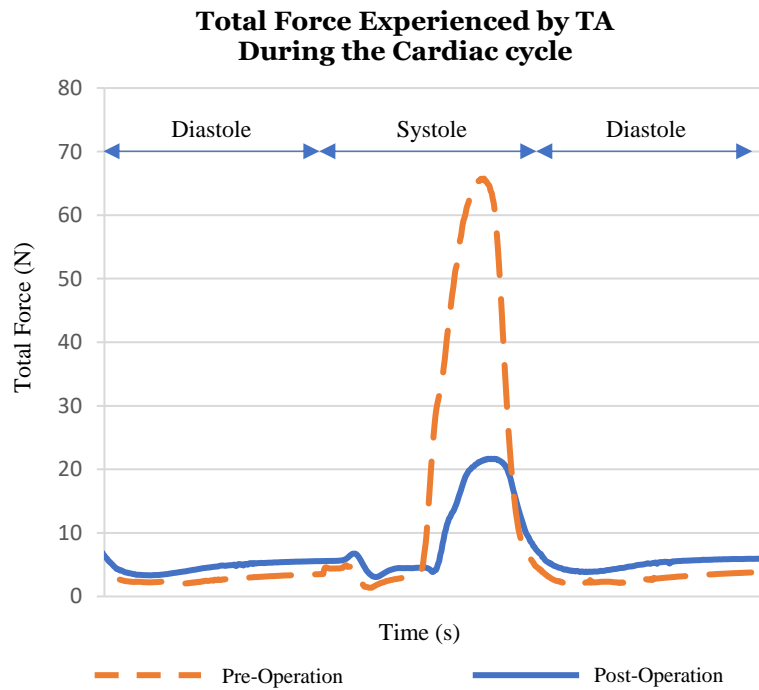


**Fig. 6** Comparison of forces on the TA shows a higher diastolic force post-operatively suggesting TA dilation is more likely. Reduced force during systole also suggests a loss of the role of the TA in coaptation.

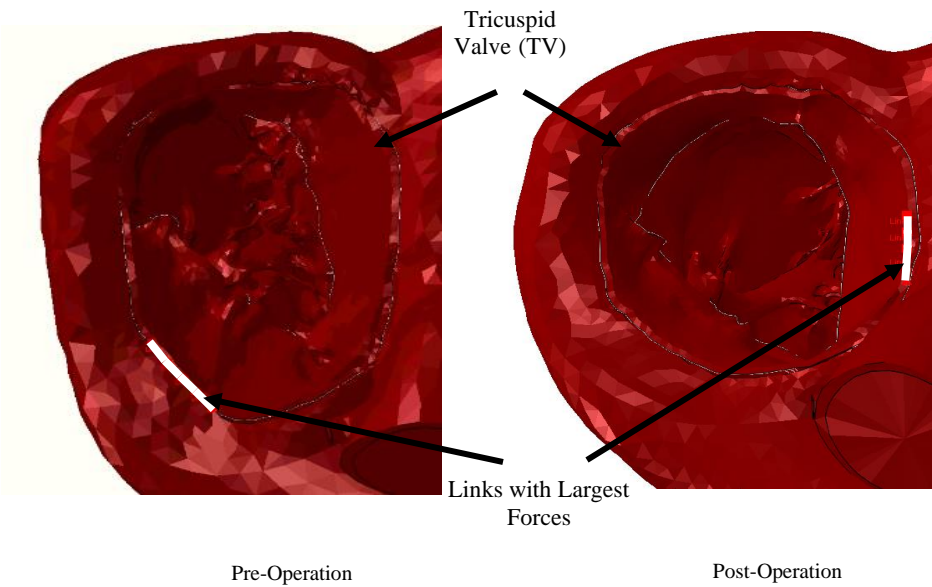


**Fig. 7** The location of the TA sections exhibiting the largest forces in pre-operative and post-operative geometries. (white).

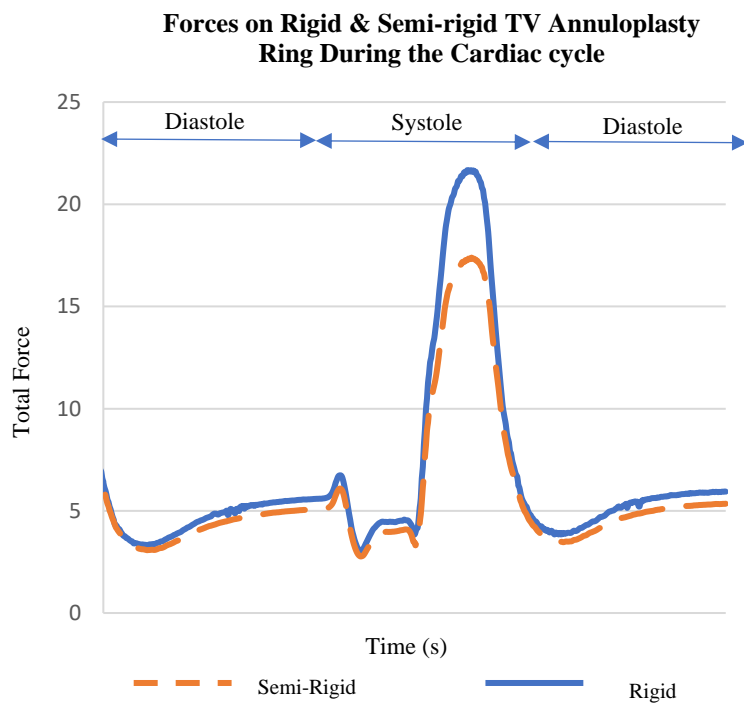


**Fig. 8** A graph of total forces on rigid and semi-rigid rings shows a reduction of forces during the contraction, reflecting a reduced likelihood of dehiscence – or suture would trauma.

**Table:**

	Constraint Type	Max. (N)	Min. (N)	Average (N)
Pre-Operative	Rigid	65.54	1.38	12.05
Post-Operative	Rigid	21.67	3.06	7.50
	Semi-Rigid	17.39	2.77	6.48

**Table 1** Breakdown of Total Forces on Pre-Operative and Post-Operative Geometries.



**Alireza Heidari, Ph.D.**

Research Associate,

Department of Mathematics and Statistics, Faculty of Science  
Department of Anatomy and Cell Biology, Faculty of Medicine

Tel: (514) 962-2600  
Fax: (514) 398-5047  
alireza.heidari@mcgill.ca

McGill University  
Burnside Hall, #1244  
805 Sherbrooke Street West  
Montreal, QC, H3A 0B9, Canada

July 15, 2020

**RE: Consent for article submission**

Dear Editor(s),

This letter is to confirm that I agree to be a corresponding author, to submit the attached manuscript entitled: "**Patient-specific Finite Element Analysis of the Human Heart: Mitral valve replacement and Tricuspid valve repair**" for consideration of publication in the **Journal of Biomechanics**. I also confirm that there are no conflict of interest, financial or otherwise, concerning the research involved with our manuscript.

I also acknowledge all our co-authors for their contributions in this paper from one direction to another.

Sincerely yours,

A handwritten signature in blue ink, appearing to read "A.H." followed by a stylized surname.

Alireza Heidari, Ph.D.



Hojatollah Vali, Ph.D.

Professor of Biomineralogy,  
Department of Anatomy & Cell Biology,  
Director, Emeritus  
Facility for Electron Microscopy Research  
McGill University

Tel: (514) 398-3025  
Fax: (514) 398-5047  
[hojatollah.vali@mcgill.ca](mailto:hojatollah.vali@mcgill.ca)

July 16, 2020

Ref.: Letter of Agreement

To whom it may concern,

This is to confirm that I agree with the submission of the manuscript entitled "*Patient-Specific Finite Element Analysis of the Human Heart: Mitral Valve Replacement and Tricuspid Valve Repair*" to the Journal of Biomechanics.

I also confirm that there are no conflict of interest concerning the research involved with this manuscript

Sincerely yours,

A handwritten signature in black ink, appearing to read "H. Vali".

Hojatollah Vali



**Dominique Shum-Tim, M.D., C.M., M.Sc., C.S.P.Q., F.R.C.S.C., F.A.C.S., F.A.H.A., F.C.C.S.**

Professeur

Division de la Chirurgie Cardiaque

Université McGill

Tel : (514) 934-1934 ext. 36873

Professor

Division of Cardiac Surgery

McGill University

Fax : (514) 843-1602

July 16<sup>th</sup>, 2020.

**Re: Letter of agreement**

Dear Editor,

This letter is to notify my agreement as a co-author, to submit the attached manuscript entitled: "**Patient-specific Finite Element Analysis of the Human Heart: Mitral valve replacement and Tricuspid valve repair**" for consideration of publication in the **Journal of Biomechanics**. I, hereby, declared that I have no conflict of interest, financial or otherwise.

I also acknowledge the contributions of each and every one of the co-authors in this paper for their valuable opinions and suggestions.

Yours sincerely,

A handwritten signature in blue ink, appearing to read "D. Shum-Tim".

D. Shum-Tim, M.D., C.M., MSc., CPSQ., FRCSC., FAHA., FACS., FCCS.  
Professor,  
Department of Surgery  
Department of Pediatric Surgery  
McGill University Health Center  
McGill University  
1001 Decarie Boulevard,  
Room C 07.1284.5  
Montreal, Quebec,  
Canada, H4A 3J1  
Tel: 514-934-1934 x36873  
Fax: 514-843-1602

July 13, 2020.

Re: Letter of agreement

Dear Editor,

I am writing this letter to document my agreement as a co-author to the submission entitled **“Patient-specific Finite Element Analysis of the Human Heart: Mitral valve replacement and Tricuspid valve repair”** for publication in the **Journal of Biomechanics (Elsevier)**. I, hereby, declare that I have no conflict of interest, financial or otherwise.

Yours sincerely,

Cristina Pop, M.D., C.M. candidate  
Department of Medicine  
Faculty of Medicine  
McGill University

A handwritten signature in black ink that reads "Cristina Pop".

### Letter of Agreement

Dear Editor,

This letter is to notify my agreement as a co-author, to submit the attached manuscript entitled: "**Patient-specific Finite Element Analysis of the Human Heart: Mitral valve replacement and Tricuspid valve repair**" for consideration of publication in the **Journal of Biomechanics**. I, hereby, declare that I have no conflict of interest, financial or otherwise.



Khalil I. Elkhodary

Associate Professor of Computational Mechanics  
The Department of Mechanical Engineering  
The American University in Cairo

**Letter of Agreement**

Dear Editor,

This letter is to notify my agreement as a co-author, to submit the attached manuscript entitled: "**Patient-specific Finite Element Analysis of the Human Heart: Mitral valve replacement and Tricuspid valve repair**" for consideration of publication in the **Journal of Biomechanics**. I, hereby, declare that I have no conflict of interest, financial or otherwise.

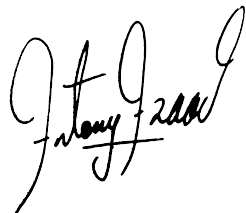


Yousof Abdel-Raouf  
Graduate Student & Research Assistant  
The Department of Mechanical Engineering  
The American University in Cairo

**Letter of Agreement**

Dear Editor,

This letter is to notify my agreement as a co-author, to submit the attached manuscript entitled: "**Patient-specific Finite Element Analysis of the Human Heart: Mitral valve replacement and Tricuspid valve repair**" for consideration of publication in the **Journal of Biomechanics**. I, hereby, declare that I have no conflict of interest, financial or otherwise.



Antony Youssef  
Research Assistant  
The Department of Mechanical Engineering  
The American University in Cairo

**Letter of Agreement**

July 13, 2020

I would like to state as co-author that I agree on submitting the paper entitled "**Patient-Specific Finite Element Analysis of the Human Heart: Mitral Valve Replacement and Tricuspid Valve Repair**" to the Journal "**Journal of Biomechanics**".

I also certify that I have no conflict of interest either financial or otherwise.

Mohamed Badran, PhD.

A handwritten signature in blue ink, appearing to read "Mohamed Badran".

Assistant Professor  
Mechanical Engineering Department  
Faculty of Engineering and Technology  
Future University in Egypt



Masoud Asgharian, PhD  
Full Professor  
Department of Mathematics and Statistics  
Burnside Hall, Room 1224  
805 Sherbrooke Street West  
Montreal, QC, Canada, H3A 0B9  
[masoud.asgharian2@mcgill.ca](mailto:masoud.asgharian2@mcgill.ca)

The Editor(s) of the *Biomechanics* journal

July 12, 2020

**RE: Consent for article submission**

Dear Editor(s),

I am writing to document my consent to the submission of our manuscript entitled "*Patient-Specific Finite Element Analysis of the Human Heart: Mitral Valve Replacement and Tricuspid Valve Repair*" to the *Biomechanics* journal. Further to my consent for submitting the aforementioned article by Dr. A. Heidari, I add that I have no conflict of interest, financial or otherwise.

Sincerely,

A handwritten signature in black ink, appearing to read "Masoud Asgharian".

Masoud Asgharian